

Abstract

The optimization calculations are made to find the optimum properties of combined quadrupole lens which consists of electrostatic and magnetic lens. The optical properties are computed, where both the focal length and the magnification are determined. Both chromatic and spherical aberration coefficients are reduced to minimum values and the achromatic aberration are found for many cases.

This calculation are achieved with the aid of transfer matrices method and using both rectangular and bell-shaped models of field distribution, where the path of charged-particles beam transversing the field has been determined by solving the trajectory equation of motion and then the optical properties for lens have been computed with the aid of the beam trajectory along the lens axis.

The computations have been concentrated on determined the focal length, magnification and chromatic and spherical aberration coefficients in both convergence and divergence planes and also, the effects of changing both of excitation and effective length of lens are studied and are taken into account.

Acknowledgments

Praise be to ALLAH, Lord of the whole creation and peace be upon his messenger Mohammad.

I would like to express my sincere thanks and deep gratitude to my supervisors **Dr. Fatin Abdul Jalil Al-Moudarris** for suggesting the present project, and **Dr. Uday Ali Al-Obaidy** for completing the present work and for their support and encouragement throughout the research.

I am most grateful to the Dean of College of Science and Head and the staff of the Department of Physics at Al-Nahrain University,

The assistance given by the staff of the library of the College of Science at Baghdad University is highly appreciated.

I acknowledge the helpful comments assistance given to me at various stage of this work by Mr. Ibrahim A.M.Al-saadi and Ms. Basma H. Al-Shamari.

Finally, I most grateful to my **parents**, my brothers **Ali, Mohanad**, and **Mostafa**, and my sisters **Shatha, Zainab**, and **Shahad** for their patience and encouragement throughout this work, and to my friends **Sura Allawi, Zeena Mowafaq**, and **Noor Mohammad**, , for their encouragement, and to **Hussain Ali**, and **Mohammad Salam** for their support.

Fatma

Certification

We certify that this thesis entitled “**Investigation of The Optical Properties of The Achromatic Quadrupole Lens**” is prepared by **Fatma Nafaa Gaafer Al-Zubaidy** under our supervision at the College of Science of Al-Nahrain University in partial fulfillment of the requirements for the degree of **Master of Science in Physics**.

Signature:

Name: Dr. Fatin A. J. Al-Moudarris

Title: (Supervisor)

Date: / / 2007

Signature:

Supervisor: Dr. Uday A. H. Al-baidy

Title: Lecturer

Date: / / 2007

In view of the recommendations, we present this thesis for debate by the examination committee.

Signature:

Name: Dr. Ahmad K. Ahmad

(Assist. Prof.)

Head of Physics Department

Date: / / 2007

1- INTRODUCTION

1-1 Electrostatic And Magnetic Quadrupole Lenses

The quadrupole lenses for focusing charged particle beams is due to the fact that quadrupole lens systems can converge the beam in all directions, even though the individual lenses cause the beam to diverge in certain directions. If the xz plane of the lens collects the charged particles, the yz plane will cause them to diverge, i.e., the quadrupole lens is astigmatic [Baranova and Yavor 1984].

The quadrupole lens systems are formed by aligned cylindrical electrodes which are cut by longitudinal slots into four equal parts to create a quadrupole lens. In order to enclose the region where the electrostatic field distribution is to be computed there are two additional long cylinders of the same diameter at both sides of the system terminated by disks at their ends. The diameter of the cylinders is taken to be the unit of length [Baranova and Read 2001]. A combined electrostatic and magnetic quadrupole lens is shown in figure (1-1). It consists of four electrodes and four magnetic poles. The solid and broken lines show the electrostatic and magnetic lines of force [Szilagyi 1988].

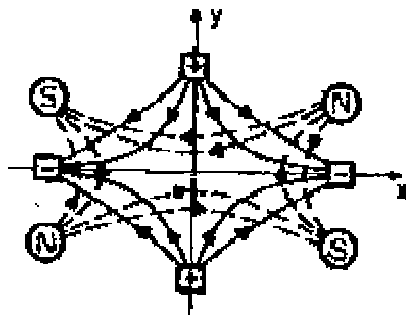


Figure (1-1): Combined electrostatic and magnetic quadrupole lens [Szilagyi 1988].

Electric and magnetic lenses can be used for focusing beams of charged particles. Each of the quadrupoles focus the beam of ions in one transverse direction and defocus it in the other. The net effect on the beam after traveling through the system is focusing in all directions. Particle tracing of the ions is used to investigate the focusing effect for the quadrupole.

The symmetry plane of the electric field of such a compound quadrupole lens is placed in coincidence with the plane of antisymmetry of the magnetic field. Electrostatic and magnetic quadrupole lenses have found application in the focusing of charge particle, in particular of high energy particles [Yavor et al 1964].

Electric quadrupole are assembled with the converging principle section of the electric lens coincident with diverging section of the magnetic lens. If the lens excitations are adjusted so that the magnetic force is everywhere twice the electric force in magnitude, the focal length is independent of particle energy [Martin and Goloskie 1982].

Quadrupole lenses are very suitable for forming a fine linear beam and a spot beam [Okayama 1989]. They are commonly used for focusing electron and ion beams of high energy. An example of such device is the ion implantation [Baranova and Read 1998]. There are many electron and ion optical instruments and devices in which there are advantages in using quadrupole lenses rather than round lenses, such as instruments where strong focusing or astigmatic properties are needed. Among these are the accelerators, electron and mass spectrometers, cathode-ray tubes and devices for correcting

aberrations. Electrostatic quadrupole lenses are often preferable to magnetic ones for focusing beams of moderate energy. They are also preferable for dealing with ion beams since the focal length of an electrostatic lens does not depend on the charge to mass ratio as it does for a magnetic lens. It seems that quadrupole lens systems are more sensitive to mechanical defects than round lens [Baranova and Read 2001]. One possible application of quadrupole lenses is to correct aberration in combination with octupole [Baranova and Yavor 1984].

1-2 Achromatic Quadrupole Lens

An achromatic quadrupole lens is formed by the electrostatic and magnetic fields imposed on each other. The compound lens thus obtained possesses first order focussing properties of an ordinary quadrupole lens, however depending upon the actual electrostatic and magnetic field strengths it may both be achromatic and exhibit negative chromatic aberration [Yavor et al 1964].

Achromatic quadrupole lenses to overcome the limitation due to energy spread. These lenses require both magnetic and electrostatic focusing elements [Harriott et al 1990].

The basing achromatic four-pole lenses on multipole lenses with several planes of symmetry and antisymmetry. Such lenses are applied, for instance, to correct aberration of various origins. Similarly to a four pole lenses, an achromatic multipole lens consists of matched electrostatic and magnetic lenses. The position and polarity of the electrode and poles are shown in figure (1-2) where an 8-pole matched lens is given as an example. As can be seen from the

diagram, the symmetry planes of the electrostatic field are matched with the antisymmetry field of the magnetic field and in these planes the forces acting on a charge particle from both fields are directed towards one another [Yavor and Dymnikov 1964].

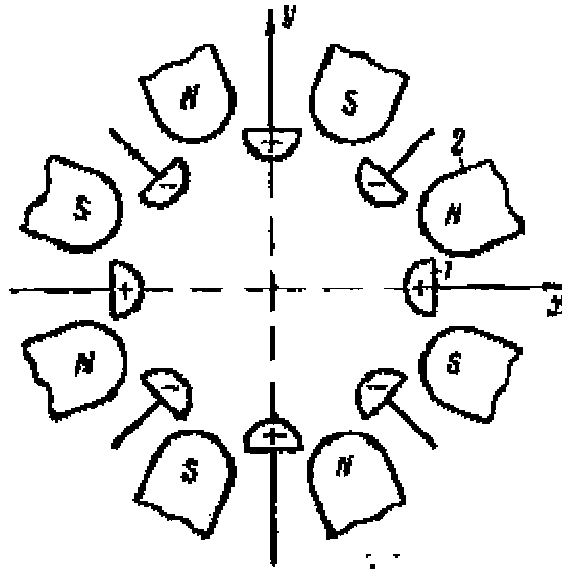


Figure (1-2): Matched 8-pole lenses. (1) electrode (2) magnetic pole. Polarity of the poles and electrodes corresponds to the motion of the charge particle in the direction of the z -axis [Yavor and Dymnikov 1964].

Achromatic operation of the lens was tested by measuring the beam width as the ion energy was varied over a wide range [Martin and Goloskie 1982]. The possibility to use achromatic quadrupole lenses for probe forming of high resolution microbeams is reviewed by Tapper [1991]. To measure the harmonic contamination in an achromatic lens the grid shadow method has to be utilized. The grid shadow pattern can also guide during the alignment of the lenses.

The achromatic quadrupole lenses were found to be an order of magnitude less sensitive to changes in the beam energy away from the operating energy compared to the equivalent magnetic or electrostatic quadrupole lenses [Jamieson and Tapper 1989].

The chromatic aberration of conventional electron lenses can never vanish, and the same is true of electrostatic and magnetic quadrupoles. If, however, we build a composite quadrupole, consisting of four electrodes with fourpole-pieces placed midway between them, the combined lens will be achromatic if the magnetic and electric excitations are suitable chosen. This was first shown by Kel'man and Yavor [1961], by deriving the condition for achromatism from paraxial equations of motion, on the assumption that the electrostatic and magnetic potentials are distributed along the axis z , in exactly the same way. This result was independently confirmed by Septier [1963], who derived the achromatic condition for potential distributions of rectangular shape. Yavor [1962] recapitulated the analysis, and Kel'man and Yavor [1963] showed that the aberration could not only be eliminated, but could take negative values [Hawkes 1965].

The first order chromatic aberration can be reduced using combined electrostatic and magnetic quadrupole whose excitations are connected by the achromatic condition. This method involves magnetic elements and leads to a complicated construction of the focusing system [Baranova and Read 1999].

1-3 Historical Development

Such a system of quadrupole lenses can be used in an electron or ion microscope, where it would be interesting to use it because of the possibility of decreasing the spherical and chromatic aberrations [Dymnikov et al 1963].

Kel'man and Yavor [1961], derived the condition for achromatism from the paraxial equations of motion, on the assumption that the electrostatic and magnetic potentials are distributed along the axis, z , in exactly the same way. This result was independently confirmed by Septier [1963], who derived the achromatic condition for potential distributions of rectangular shape. Yavor [1962] recapitulated the analysis, and 1963, Kel'man and Yavor [1963] showed that the aberration could not only be eliminated, but could take negative values. More recently, Kel'man et al [1963] and Yavor et al [1964] published an account of their experimental work on these achromatic systems. Yavor and Dymnikov [1964] demonstrated that not composite quadrupoles, but any composite $2N$ -pole can be rendered achromatic in this way. Yavor et al [1964] considered the effect of slight differences between magnetic and electrostatic field distributions, and calculated the aperture aberrations of an achromatic composite lens [Hawkes 1965].

The effective lengths of electrostatic and magnetic lenses of these types are equal to their actual lengths [Shpak and Yavor 1965].

The electron-optical properties of short double quadrupole, hexapole, and octupole electromagnetic lenses were analyzed. Expressions were derived for the effect of these lenses on the trajectory of an electron beam. It was shown that the use of these lenses in a system for focusing and deflecting an electron beam can correct distortion, astigmatism, and coma [Markovich 1972].

The strength of an electrostatic quadrupole depends on the energy of the ion whereas the strength of a magnetic lens was determined by the momentum. As a result, the chromatic aberration of a magnetic lens was half that of the electrostatic [Grime and Watt 1988]. It was suggested by workers in the Leningrad group that this difference could be exploited to produce achromatic quadrupoles by constructing a lens which has opposing electrostatic and components, arranged so that the magnetic strength was always twice the electrostatic strength. In this way, the major chromatic effects can be cancelled out. Only one attempt to construct an achromatic lens based on this principle was reported and it was shown to be possible to cancel the chromatic aberration. The alternative approach to the elimination of chromatic aberration is to reduce the beam energy spread.

The optical properties of the new correction lens were calculated by using simulated potential distributions. Aperture aberration coefficients of the new correction lens corrected to less than 0.1mm. It was confirmed experimentally that the probe size was improved remarkably by excitations of the aperture electrodes [Okayama 1990].

The quadrupole lenses were used to modify the beam shape in order to penetrate well through the entrance slit of the magnet. The dimensions, the focal lengths, and the magnification were calculated using a matrix multiplication method. Through these calculations, the lens parameters for each quadrupole lens were determined to minimize the distortion of the image on the focal plane [shimizu et al 2000].

Charged particle beam trajectories in a simple electromagnetic quadrupole-octupole lens were numerically calculated based on analytical

expressions for the potential distribution by Ovsyannikova and Fishkova [2001] Locations of the lens foci in the image space were determined over a wide range of initial conditions. Relationships between the electrostatic and magnetic lens components that provide correction for chromatic aberrations.

The chromatic aberrations are corrected by electric and magnetic quadrupole lenses, but quadrupole – octupole correctors are well suited for correcting chromatic and spherical aberrations [Rose 2003].

The hexapole corrector has the simplest structure yet eliminates only third-order spherical aberration and coma. The quadrupole-octupole corrector eliminates chromatic aberration by means of crossed electric and magnetic quadrupoles and the third-order spherical aberration by octupoles [Rose and Wan 2005].

The quadrupole lens is more complex than the axial symmetrical, in construction, in calculations and in operation. As it is known, these lenses have found a wide application in accelerator techniques, such as the high-energy microprobe and the scanning ion microscope, where it is only necessary to focus ions into a very small spot [Dymnikov et al 2005].

1-4 The Aim Of The Project

The aim of this thesis is finding the optimum properties of combined quadrupole lens, which consists of electrostatic and magnetic lenses. The optimization role is made via testing two field distribution models, where both rectangular and bell-shaped models are used to reach to achromatic aberration and minimum spherical aberration case. The optical properties of combined quadrupole lens are computed for each model by solving the trajectory equation of charge-particles beam for both convergence and divergence planes and the transfer matrices are used to find this optical properties as focal length, magnification and aberration coefficients. The effect of the lens excitation, image and object distance and effective length of the lens on chromatic and spherical aberration coefficients are investigated to find the optimum values of these coefficients.

2- THEORETICAL CONSIDERATIONS

2-1 Field Models For Quadrupole Lenses

The field distribution of a quadrupole lens may be represented by various models shown in figure (2-1). According to [Hawkes 1965/1966] the function $f(z)$ of the field distribution can be obtained either by measurement or by computation, and it may transpire that some mathematically convenient model represents $f(z)$ sufficiently. For example, for long narrow quadrupole lenses, the rectangular model figure (2-1a) is often a close enough approximation. The function $f(z)$ for rectangular field model of axial width L is represented mathematically as follows:

$$f(z) = (f(z))_{\max} = 1 \quad \text{when } -L/2 \leq z \leq L/2 \quad (2.1)$$

At points when $|z| > L/2$ the function $f(z) = 0$. This model is also known as the square-top field distribution.

For short quadrupole lenses, Glaser's bell-shaped model figure (2-1b) is found to be more suitable and is represented by the following function,

$$f(z) = (f(z))_{\max} / [1 + (z/d)^2]^2 = 1 / [1 + (z/d)^2]^2 \quad (2.2)$$

where d is the axial extension of the field between the two points where $f(z) = (f(z))_{\max}/4$; at $z = 0$, $f(z)$ equals to unity. The value of d is determined by the shape of the electrodes.

The modified bell-shaped field model, figure (2-1c), represents the intermediate case such that the field distribution may be represented by the following function:

$$f(z) = 1/[1 + ((z - z_1)/d)^2]^2 \quad \text{when } z > z_1 \quad (2.3)$$

$$f(z) = 1/[1 + ((z + z_1)/d)^2]^2 \quad \text{when } z > -z_1 \quad (2.4)$$

The function $f(z)$ has a rectangular section of constant maximum value of $(f(z))_{\max} = 1$ in the region $-z_1 \leq z \leq z_1$ such that beyond these boundaries it terminates in the form of half bell-shaped field represented by the two equations (2.3) and (2.4).

The triangular field distribution model figure (2-1d) is another model proposed by Hawkes [1965/1966]; it is given by:

$$f(z) = \Phi_{z+z_2} \quad \text{when } -z_2 \leq z \leq 0 \quad (2.5a)$$

$$f(z) = -\Phi_z + z_2 \quad \text{when } 0 \leq z \leq z_2 \quad (2.5b)$$

$$f(z) = (f(z))_{\max} = 1 \quad \text{at } z = 0 \quad (2.5c)$$

where Φ is the slope of the two steep sides of the triangle. It should be noted that these potential distribution models are actually proposed for the hyperbolic cross-section of the quadrupole lens electrodes.

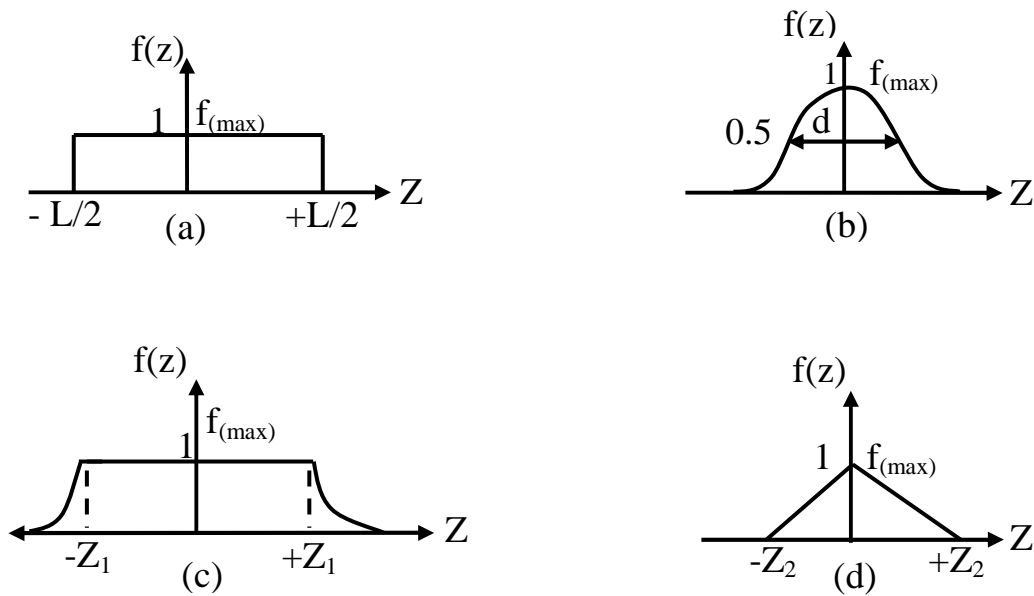


Figure (2-1): Field distribution of a quadrupole lens [Hawkes 1965/1966].

- (a) Rectangular model (b) Bell-shaped model
(c) Modified bell-shaped model (d) Triangular model.

2-2 The Paraxial Ray Equation of Motion and The First-Order Optical Properties

The paraxial ray equation in cartesian coordinates for the charged-particles beam traversing the field of a quadrupole lens are given as follows [Hawkes 1970]:

$$x'' + \beta^2 f(z) x = 0 \quad (2.6)$$

$$y'' - \beta^2 f(z) y = 0 \quad (2.7)$$

where β is the lens excitation, and k is a coefficient accounting for the shape of electrode, since the present work has been concentrated on the hyperbolic for electrodes, thus $k = 1$ [Dymnikov et al 1965 and Grivet 1972].

2-2-1 The rectangular model

The general solution of the second-order linear homogeneous differential equations (2.6) and (2.7) can always be written in the following [Hawkes 1970]

$$x = x_0 \cos(\beta z) + x'_0 (1/\beta) \sin(\beta z) \quad (2.8)$$

$$x' = -x_0 \beta \sin(\beta z) + x'_0 \cos(\beta z) \quad (2.9)$$

$$y = y_0 \cosh(\beta z) + y'_0 (1/\beta) \sinh(\beta z) \quad (2.10)$$

$$y' = y_o \beta \sinh(\beta z) + y_o' \cosh(\beta z) \quad (2.11)$$

where x_o and y_o are the initial displacements from the optical axis in the $x-z$ and $y-z$ plane respectively, and x_o' and y_o' are the initial gradients of the beam in the corresponding planes.

can always be written in the following matrix form respectively.

$$\begin{pmatrix} x(z) \\ x'(z) \end{pmatrix} = T_c \begin{pmatrix} x_o(z) \\ x_o'(z) \end{pmatrix} \quad (2.12)$$

$$\begin{pmatrix} y(z) \\ y'(z) \end{pmatrix} = T_d \begin{pmatrix} y_o(z) \\ y_o'(z) \end{pmatrix} \quad (2.13)$$

The parameter T_c and T_d are the transfer matrices in the convergence plane xoz and the divergence plane $yo z$ respectively which are given by [Larson 1981 and Szilagyi 1988].

$$T_c = \begin{pmatrix} \cos(\beta L) & 1/\beta \sin(\beta L) \\ -\beta \sin(\beta L) & \cos(\beta L) \end{pmatrix} \quad (2.14)$$

$$T_d = \begin{pmatrix} \cosh(\beta L) & 1/\beta \sinh(\beta L) \\ \beta \sinh(\beta L) & \cosh(\beta L) \end{pmatrix} \quad (2.15)$$

In practice, length L is the "effective length" which has been found experimentally to be given by [Hawkes 1970].

$$L = \ell + 1.1c \quad (2.16)$$

where ℓ is the electrode length and c is the bore radius which is assumed to be very small. According to Hawkes [1970] the coefficient 1.1 of c was measured experimentally by Septier in [1958]; however, it has been proposed theoretically by Reisman in [1957]. Therefore, the effective length L could be equal to the electrode length ℓ by neglecting the second term of equation (2.16) i.e. $L \approx \ell$ where $\theta = \beta L$ [Hawkes 1970].

All first-order optical properties of a quadrupole lens can be derived from the matrices given in equations (2.14) and (2.15). If these matrices are represented by

$$T_c = \begin{pmatrix} a_{11} & a_{12} \\ a_{21} & a_{22} \end{pmatrix} \quad (2.17a)$$

$$T_d = \begin{pmatrix} a_{11} & a_{12} \\ a_{21} & a_{22} \end{pmatrix} \quad (2.17b)$$

Then the following first-order optical properties can be determined (see figure 2-2)

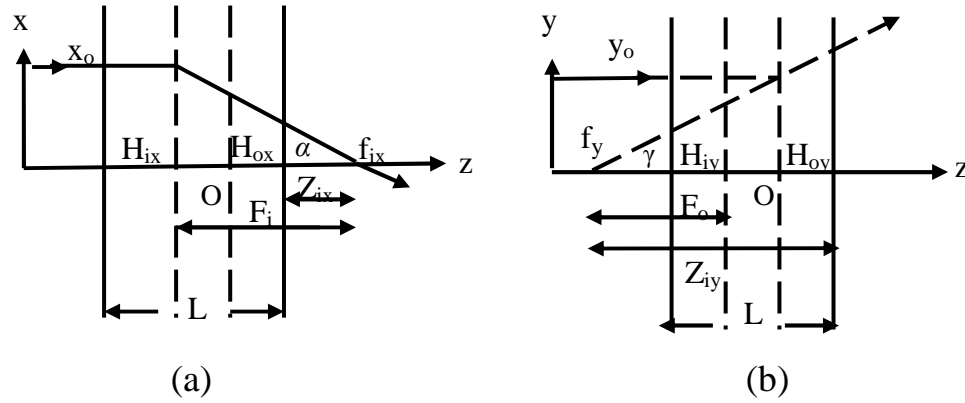


Figure (2-2) The cardinal elements of a quadrupole lens, (a) in the convergence plane, (b) in the divergence plane (Grivet 1972).

(a) focal planes

An incoming ray parallel to the optical axis will, after passing through the lens system, intersect the axis at a point whose Z_i from the exit plane is given by Grivet [1972]:

$$Z_i = - a_{11} / a_{21} \tag{2.18}$$

From equations (2.14) and (2.15)

$$Z_{ic} = \cos(\theta) / \beta \sin(\theta) \tag{2.19}$$

$$Z_{id} = -\cosh(\theta)/\beta\sinh(\theta) \quad (2.20)$$

where the subscript "i" denotes image and "c" and "d" denote the convergence and divergence planes respectively. A ray emerging parallel to the optical axis, arises from a point Z_o at the entry plane given by:

$$Z_o = -a_{22}/a_{21} \quad (2.21)$$

$$Z_{oc} = \cos(\theta)/\beta\sin(\theta) \quad (2.22)$$

$$Z_{od} = -\cosh(\theta)/\beta\sinh(\theta) \quad (2.23)$$

where the subscript "o" refers to the object

(b) principal planes

The principle planes are conjugate and can be defined as follows:

$$H_i = (1 - a_{11})/a_{21} \quad (2.24)$$

from equations (2.14) and (2.15) we can get the following relations:

$$H_{ic} = (\cos(\theta) - 1)/\beta \sin(\theta) \quad (2.25)$$

$$H_{id} = (1 - \cosh(\theta))/\beta \sinh(\theta) \quad (2.26)$$

similarly

$$H_o = (1 - a_{22})/a_{21} \quad (2.27)$$

$$H_{oc} = (\cos(\theta) - 1)/\beta \sin(\theta) \quad (2.28)$$

$$H_{od} = (1 - \cosh(\theta))/\beta \sinh(\theta) \quad (2.29)$$

(c) focal lengths

The focal length is defined as the distance between the focal point F and the corresponding principal plane. Therefore, the image-side and object-side focal lengths f_i and f_o respectively are given by:

$$f_i = f_o = -1/a_{21} \quad (2.30)$$

then

$$f_c = 1/\beta \sin\theta \quad (2.31)$$

$$f_d = -1/\beta \sinh\theta \quad (2.32)$$

(d) magnification

In any optical system the ratio between the transverse dimension of the final image and the corresponding dimension of the original object is called the magnification can be given as:

$$M = 1/a_{21} u + a_{11} \quad (2.33)$$

In the convergence and divergence planes the magnification is given by:

$$M_c = 1/\cos\theta - u \beta \sin\theta \quad (2.34)$$

$$M_d = 1/\cosh\theta + u \beta \sinh\theta \quad (2.35)$$

Where u is the object distance.

2-2-2 The bell-shaped

By using equation (2.6) and (2.7) yield with equation (2.2) to form:

$$x'' + \beta^2 / (1+(z/d)^2)^2 x = 0 \quad (2.36)$$

$$y'' - \beta^2 / (1+(z/d)^2)^2 y = 0 \quad (2.37)$$

Let the new variables p and ψ be introduced, so that one would have [Szilagyí 1988]

$$z/d = \cot(\psi) \quad (2.38)$$

and

$$x/d = p(\psi)/\sin(\psi) \quad (2.39)$$

then equation (2.36) for convergence plane can be rewritten as:

$$dp^2/d\psi + w^2 p = 0 \quad (2.40)$$

The properties of the quadrupole lens are characterized by the parameters:

$$w_c^2 = 1 - \beta^2 d^2 \quad \text{for the convergence plane}$$

and

$$w_d^2 = 1 + \beta^2 d^2 \quad \text{for the divergence plane}$$

The solution of equations (2.36) and (2.37) is elementary. Returning to the variables x and y one can write

$$x = d [x_o \cos(w_c \psi) + x'_o \sin(w_c \psi)] / \sin(\psi) \quad (2.41)$$

$$\begin{aligned} x' = & [x_o [d w_c \sin(\psi) \sin(w_c \psi) + d \cos(\psi) \cos(w_c \psi)] / \sin^2(\psi) [1 + (z/d)^2 \\ & d]] + [x'_o [d \cos(\psi) \sin(w_c \psi) - d w_c \sin(\psi) \cos(w_c \psi)] / \sin^2(\psi) \\ & [1 + (z/d)^2 d]] \end{aligned} \quad (2.42)$$

$$y = d [y_o \cos(w_d \psi) + y'_o \sin(w_d \psi)] / \sin(\psi) \quad (2.43)$$

$$\begin{aligned}
y' = & [y_o [d w_d \sin(\psi)\sin(w_d \psi) + d \cos(\psi) \cos(w_d \psi)]/\sin^2(\psi) [1+(z/d)^2] \\
& d]] + [y_o' [d \cos(\psi) \sin(w_d \psi) - d w_d \sin(\psi) \cos(w_d \psi)]/\sin^2(\psi) \\
& [1+(z/d)^2]]
\end{aligned} \tag{2.44}$$

For the second-order linear homogenous differential equations (2.36) and (2.37) the solution can be written in the following matrix form

$$\begin{pmatrix} x(z) \\ x'(z) \end{pmatrix} = T_c \begin{pmatrix} x_o(z) \\ x_o'(z) \end{pmatrix} \tag{2.45}$$

$$\begin{pmatrix} y(z) \\ y'(z) \end{pmatrix} = T_d \begin{pmatrix} y_o(z) \\ y_o'(z) \end{pmatrix} \tag{2.46}$$

Then by using equations (2.42) and (2.44), T_c and T_d become:

$$T_c = \begin{pmatrix} \frac{d \cos(w_c \psi)}{\sin(\psi)} & \frac{d \sin(w_c \psi)}{\sin(\psi)} \\ \frac{[d w_c \sin(\psi) \sin(w_c \psi) + d \cos(\psi) \cos(w_c \psi)]}{\sin^2(\psi)[1+z^2/d^2]d} & \frac{[d \cos(\psi) \sin(w_c \psi) - d w_c \sin(\psi) \cos(w_c \psi)]}{\sin^2(\psi)[1+z^2/d^2]d} \end{pmatrix} \tag{2.47}$$

$$T_d = \begin{pmatrix} \frac{d \cos(w_d \psi)}{\sin(\psi)} & \frac{d \sin(w_d \psi)}{\sin(\psi)} \\ \frac{[d w_d \sin(\psi) \sin(w_d \psi) + d \cos(\psi) \cos(w_d \psi)]}{\sin^2(\psi)[1 + z^2/d^2]d} & \frac{[d \cos(\psi) \sin(w_d \psi) - d w_d \sin(\psi) \cos(w_d \psi)]}{\sin^2(\psi)[1 + z^2/d^2]d} \end{pmatrix} \quad (2.48)$$

Then the following first order optical properties can be determine:

(a) focal planes

From equations (2.47) and (2.48)

$$Z_{ic} = -\frac{d^2 \cos(w_c \psi) \sin^2(\psi)[1 + (z/d)^2]}{\sin(\psi)[d w_c \sin(\psi) \sin(w_c \psi) + d \cos(\psi) \cos(w_c \psi)]} \quad (2.49a)$$

$$Z_{id} = -\frac{d^2 \cos(w_d \psi) \sin^2(\psi)[1 + (z/d)^2]}{\sin(\psi)[d w_d \sin(\psi) \sin(w_d \psi) + d \cos(\psi) \cos(w_d \psi)]} \quad (2.49b)$$

$$Z_{oc} = -\frac{d \cos(\psi) \sin(w_c \psi) - d w_c \sin(\psi) \cos(w_c \psi)}{d w_c \sin(\psi) \sin(w_c \psi) + d \cos(\psi) \cos(w_c \psi)} \quad (2.49c)$$

$$Z_{od} = -\frac{d \cos(\psi) \sin(w_d \psi) - d w_d \sin(\psi) \cos(w_d \psi)}{d w_d \sin(\psi) \sin(w_d \psi) + d \cos(\psi) \cos(w_d \psi)} \quad (2.49d)$$

(b) principal planes

From equations (2.47) and (2.48) we can get the following relations:

$$H_{ic} = \frac{\sin^2(\psi)[1 + (z/d)^2]d}{[d w_c \sin(w_c \psi) + d \cos(\psi) \cos(w_c \psi)]} \left[1 - \frac{d \cos(w_c \psi)}{\sin(\psi)}\right] \quad (2.50a)$$

$$H_{id} = \frac{\sin^2(\psi)[1 + (z/d)^2]d}{[d w_d \sin(w_d \psi) + d \cos(\psi) \cos(w_d \psi)]} \left[1 - \frac{d \cos(w_d \psi)}{\sin(\psi)}\right] \quad (2.50b)$$

$$H_{oc} = \frac{[\sin^2(\psi)[1 + (z/d)^2]d - [d \cos(\psi) \sin(w_c \psi) - d w_c \sin(\psi) \cos(w_c \psi)]]}{[d w_c \sin(\psi) \sin(w_c \psi) + d \cos(\psi) \cos(w_c \psi)]} \quad (2.50c)$$

$$H_{od} = \frac{[\sin^2(\psi)[1 + (z/d)^2]d - [d \cos(\psi) \sin(w_d \psi) - d w_d \sin(\psi) \cos(w_d \psi)]]}{[d w_d \sin(\psi) \sin(w_d \psi) + d \cos(\psi) \cos(w_d \psi)]} \quad (2.50d)$$

(c) focal lengths

From equations (2.47) and (2.48)

$$f_c = -\frac{\sin^2(\psi)[1 + (z/d)^2]d}{[d w_c \sin(\psi) \sin(w_c \psi) + d \cos(\psi) \cos(w_c \psi)]} \quad (2.51a)$$

$$f_d = -\frac{\sin^2(\psi)[1 + (z/d)^2]d}{[d w_d \sin(\psi) \sin(w_d \psi) + d \cos(\psi) \cos(w_d \psi)]} \quad (2.51b)$$

(d) magnification

$$M_c = \frac{1}{\frac{d w_c \sin(\psi) \sin(w_c \psi) + d \cos(\psi) \cos(w_c \psi)}{\sin^2(\psi)[1 + (z/d)^2]} d} u + \frac{d \cos(w_c \psi)}{\sin(\psi)} \quad (2.52a)$$

$$M_d = \frac{1}{\frac{d w_d \sin(\psi) \sin(w_d \psi) + d \cos(\psi) \cos(w_d \psi)}{\sin^2(\psi)[1 + (z/d)^2]} d} u + \frac{d \cos(w_d \psi)}{\sin(\psi)} \quad (2.52b)$$

2-3 Lens Aberration Parameters

In an ideal optical system, all rays of light from a point in the object plane would converge to the same point in the image plane, forming a clear image. The influences which cause different rays to converge to different points are called aberrations. Thus aberration can be defined as the defect that the image suffers from, when it is formed by an optical device (single or system of lenses). The aberration is a subject of great importance, since it causes limitation to the performance of various electron optical elements and systems.

Aberrations are what we call the errors our simple view of a lens gives compared to reality. Therefore, The aberrations that affect the quality of the image formed by an electron lens depend critically upon the nature of the object [Hawkes 1967].

Error may occur from different velocities that the charged particles may have in the accelerated beam since they leave the source with different initial velocities (energy spread). The result is that different particles(ions or electrons) are focused at different points even if the paraxial approximation is exactly valid. The reason of this effect is that the imaging field less influences

the particles with high initial energy than lower-energy particles. Aberration is not the only defect that the image suffers from. Other type of defects are due to the fabrication of lenses such as mechanical imperfection and misalignment. The electrostatic repulsion forces between particles of the same charge causes a deviation in charged particles path. It is another defects, known as the space charge effect, and it is a case of charged-particle optics alone that cannot be found in light optics [Szilagyí 1988].

However, in the present work attention is paid only on the two main aberrations, namely spherical aberration and chromatic aberration due to their significant effect in various ion and electron optical systems.

The reduction of both chromatic and aperture aberrations of stigmatic as well as astigmatic images formed by a doublet of electrostatic crossed aperture lenses [Baranova and Read 1998].

It has been shown that the aberration of the system can be decreased with the asymmetrization of the quadrupole lens. This result was proved by numerical calculations carried out for the "rectangular model". It is pointed out that it is possible to apply the asymmetrization in energy and mass spectrometers in order to improve the resolution of the system [Szabo 1975].

In the majority of cases the quality of electron optical devices is determined by the spherical and chromatic aberrations of the fields involved. It is known that in axially symmetric lenses these kinds of aberration cannot be eliminated in principle. In connection with this, the investigation of the spherical aberration of compound (that is, composed of electrostatic and magnetic) quadrupole lenses becomes particularly interesting [Dymnikov et al 1965].

The chromatic and spherical aberrations of round lenses together, as the pair of defects that quadrupoles can conveniently correct. The chromatic effects of quadrupoles are often considered separately from the aperture aberrations [Hawkes 1970]. The possibility of correction of aberrations in a system by octupoles is investigated by Yavor et al [1972].

The correction of both chromatic and spherical aberration becomes mandatory at voltages below 10 kV because the chromatic aberration increases rapidly with decreasing energy whereas the spherical aberration does not [Rose and Wan 2005].

2-3-1 Chromatic aberration

Chromatic aberrations are due to the fact that refractive index is actually a function of the wavelength of the light.

The possibility of correcting chromatic aberrations was introduced by Scherzer [1947] and achromatic systems with coincident magnetic and electrostatic quadrupoles were later proposed by Kel'man and Yavor [1961] and Septier [1963]. Chromatic aberration correction is promising for low voltage applications, but it may not be possible to obtain the electric fields necessary for its use in high voltage electron microscopy [Moses 1971].

Quadrupole lens systems differ from round lenses in that their chromatic aberration coefficients can be reduced to zero or made negative, provided that both electrostatic and magnetic quadrupoles are present. It is thus possible, in principle at least, to construct achromatic quadrupole multiplets and to design quadrupole correctors that can cancel the chromatic aberration of round lenses [Hawkes 1970].

Quadrupole lenses also suffer from chromatic aberration owing to the finite energy spread of the beam. In principle chromatic aberration can be reduced by improvement in the energy stabilization of the accelerator used to provide the beam [Jamieson and Legge 1987].

The chromatic aberration coefficients, defined by [Hawkes 1970]:

$$\Delta X(z_i) = M_c (Ccx\alpha + Cmx x_o) \frac{\Delta V}{V} \quad (2.53)$$

$$\Delta Y(z_i) = M_d (Ccy\gamma + Cmy y_o) \frac{\Delta V}{V} \quad (2.54)$$

where x_o and y_o are the initial displacements from optical axis in the x-z plane and y-z plane, respectively; α and γ are the image side semi-aperture angles in the x-z and y-z planes, respectively.

2-3-1-1 rectangular model

The coefficients of chromatic aberration in a rectangular model field is given by [Hawkes 1970]:

$$\frac{Ccx}{L} = \frac{n-1}{4 \sin^2(\theta)} \left[\left(1 + \frac{\sin(2\theta)}{2\theta}\right) (m_c^2 + 1) - 2 \left(\cos(\theta) + \frac{\sin(\theta)}{\theta}\right) m_c \right] \quad (2.55)$$

$$\frac{Ccy}{L} = -\frac{n-1}{4 \sinh^2(\theta)} \left[\left(1 + \frac{\sinh(2\theta)}{2\theta}\right) (m_d^2 + 1) - 2 \left(\cosh(\theta) + \frac{\sinh(\theta)}{\theta}\right) m_d \right] \quad (2.56)$$

$$C_{mx} = -\frac{n-1}{4} \frac{\theta}{\sin(\theta)} \left[\left(1 + \frac{\sin(2\theta)}{2\theta}\right) m_c - \left(\cos(\theta) + \frac{\sin(\theta)}{\theta}\right) \right] \quad (2.57)$$

$$C_{my} = -\frac{n-1}{4} \frac{\theta}{\sinh(\theta)} \left[\left(1 + \frac{\sinh(2\theta)}{2\theta}\right) m_d - \left(\cosh(\theta) + \frac{\sinh(\theta)}{\theta}\right) \right] \quad (2.58)$$

where $n = \frac{\beta e^2}{\beta^2} = \frac{\beta e^2}{\beta m^2 - \beta e^2}$ and βe and βm are the excitation of electric and magnetic lenses respectively.

2-3-1-2 bell-shaped model

The coefficients of chromatic aberration in a bell-shaped model field is given by [Hawkes 1970]:

$$\frac{C_{cx}}{d} = -\frac{n-1}{8} \frac{\beta^2 d^2}{\sin(\pi w_c)^2} \left[\left(\frac{\sin(2\pi w_c)}{w_c} - 2\pi \right) (m_c^2 + 1) + 4m_c \left(\frac{\sin(\pi w_c)}{w_c} - \pi \cos(\pi w_c) \right) \right] \quad (2.59)$$

$$\frac{C_{cy}}{d} = \frac{n-1}{8} \frac{\beta^2 d^2}{\sin(\pi w_d)^2} \left[\left(\frac{\sin(2\pi w_d)}{w_d} - 2\pi \right) (m_d^2 + 1) + 4m_d \left(\frac{\sin(\pi w_d)}{w_d} - \pi \cos(\pi w_d) \right) \right] \quad (2.60)$$

$$C_{mx} = \frac{n-1}{8} \frac{\beta^2 d^2 f_c}{w_c^2 d} \left[\left(\frac{\sin(2\pi w_c)}{w_c} - 2\pi \right) m_c + 2 \left(\frac{\sin(\pi w_c)}{w_c} - \pi \cos(\pi w_c) \right) \right] \quad (2.61)$$

$$C_{my} = -\left[\frac{n-1}{8} \frac{\beta^2 d^2 f_d}{w_d^2 d} \left[\left(\frac{\sin(2\pi w_d)}{w_d} - 2\pi \right) m_d + 2 \left(\frac{\sin(\pi w_d)}{w_d} - \pi \cos(\pi w_d) \right) \right] \right] \quad (2.62)$$

where $d = \frac{2L}{\pi}$ and L is effective length of lens.

2-3-2 Spherical aberration

Spherical aberration is the name given to the effect where the focal length of a lens will vary depending on how far you are from the centre of the lens. What this means in reality is that a parallel ray of light entering the lens near the centre of the lens will be focussed less or more than a parallel ray entering near the edges of the lens.

Scherzer [1936] showed that any combination of rotationally symmetric magnetic and electrostatic lenses has a nonzero aperture aberration. Tretner [1959] determined the lower bounds for these aberrations. Scherzer [1947] also demonstrated that third order aperture aberrations can be eliminated by combining quadrupole and octupole lenses with rotationally symmetric lenses [Moses 1970].

The aperture aberrations of quadrupoles depend upon the object position in a particularly simple way [Hawkes 1967/1968].

Values of geometrical aberration coefficients of quadrupole lenses are calculated for different focal lengths. The calculation was performed for lenses where the field along the optical axis may be approximated by a rectangle. The results are compared with those for axially-symmetric lenses. Geometrical aberrations of oblique beams in electron-optical systems become very

significant when it is desirable to use a wide field of view [Ovsyannikova 1968].

The spherical aberration coefficients, defined by [Hawkes 1970]:

$$\Delta X(z_i) = M_c (C_{30} \alpha^3 + C_{12} \alpha \gamma^2) \quad (2.63)$$

$$\Delta Y(z_i) = M_d (D_{03} \gamma^3 + D_{21} \alpha^2 \gamma) \quad (2.64)$$

The coefficients C characterize the aberration in convergence plane, and D in the divergence plane.

2-3-2-1 rectangular model

The coefficients of spherical aberration in a rectangular model field is given by [Fishkova et al 1968]:

$$\begin{aligned} \frac{C_{30}}{L} = & \frac{1}{16} [\eta^2 - (1 - 6\mu^2 + \mu^4) \left(\frac{\sin 4\theta}{4\theta} \right) + \left(\frac{u}{L} \right) \xi (1 - \cos 4\theta) + \frac{1}{3} (2 - 2n + 3n^2) [3\eta^2 - 4(1 - \mu^4) \\ & \left(\frac{\sin 2\theta}{2\theta} \right) + (1 - 6\mu^2 + \mu^4) \left(\frac{\sin 4\theta}{4\theta} \right) + 4 \left(\frac{u}{L} \right) \eta (1 - \cos 2\theta) - \left(\frac{u}{L} \right) \xi (1 - \cos 4\theta)] \end{aligned} \quad (2.65)$$

$$\begin{aligned} \frac{C_{12}}{L} = & \frac{1}{16} [6\eta\xi + 8 \left(\frac{u}{L} \right) - [2\xi^2 + (5\xi\eta - 4\mu^2) \cosh 2\theta] \left(\frac{\sin 2\theta}{2\theta} \right) + [2\eta^2 - (\xi\eta + 20\mu^2) \cos 2\theta] \\ & \left(\frac{\sinh 2\theta}{2\theta} \right) - 2 \frac{u}{L} (\xi \cos 2\theta - \eta \cosh 2\theta) + \frac{u}{L} (\eta - 5\xi) \sin 2\theta \sinh 2\theta - \frac{u}{L} (5\eta + \xi) \\ & \cos 2\theta \cosh 2\theta + (2 + 2n - n^2) [-2\eta\xi - 2 \frac{u}{L} + [2\xi^2 - (\eta\xi - 4\mu^2) \cosh 2\theta] \left(\frac{\sin 2\theta}{2\theta} \right) \\ & + [2\eta^2 - (\eta\xi + 4\mu^2) \cos 2\theta] \left(\frac{\sinh 2\theta}{2\theta} \right) + 2 \frac{u}{L} (\xi \cos 2\theta + \eta \cosh 2\theta) \\ & + \frac{u}{L} (\eta - \xi) \sin 2\theta \sinh 2\theta - \frac{u}{L} (\eta + \xi) \cos 2\theta \cosh 2\theta] \end{aligned} \quad (2.66)$$

The coefficients C characterize the aberration in the convergence plane, and D in the divergence plane.

where $\mu = \beta u$, $\eta = 1 + \mu^2$, and $\xi = 1 - \mu^2$

The coefficients D_{03} and D_{21} are derived from equations (2.65) and (2.66) by replacing β by $i\beta$.

2-3-2-2 bell-shaped model

Coefficients of spherical aberration are given in the short lens approximation. Analytical expressions were obtained for the coefficients of spherical aberration for a bell-shaped field distribution. In the case of a doublet consisting of two compound lenses with a bell-shaped field distribution it is possible to compensate the spherical aberration of the width of a linear image over all its length [Dymnikov et al 1965].

The analytical expressions for aberration coefficients of quadrupole lenses with bell-shaped axial field distribution were calculated. The calculation was carried out for an astigmatic beam. The position of the object was at the focus of the converging plane [Szilagyi et al 1973].

The coefficients of spherical aberration in a bell-shaped field is given by [Dymnikov et al 1965]:

$$\frac{C_{30}}{d} = \frac{1}{32 \sin^4 \psi_0} [(w_c^2 - 1)(w_c^2 + 3) \frac{\pi}{w_c^5} + \frac{2(7 - w_c^2)}{4w_c^2 - 1} (\sin 2\psi_0 - \sin 2\psi_1) + (2 - 2n + 3n^2) (w_c^2 - 1) [\frac{\pi}{w_c^5} - \frac{2}{4w_c^2 - 1} (\sin 2\psi_0 - \sin 2\psi_1)]] \quad (2.67)$$

$$\begin{aligned}
\frac{C_{12}}{d} = & \frac{1}{32w_d^2 \sin^4 \psi_0} [[-4[(1 - \cos 2\pi \frac{w_d}{w_c}) \sin 2\psi_1 + w_d(1 - \cos 2\psi_1) \sin 2\pi \frac{w_d}{w_c}] + 3 \\
& (w_c^2 - 1)[-2(w_c^2 - 1) \frac{\pi}{w_c^3} + \frac{1}{w_c^2 - 1} [-\frac{w_d^2(w_c^2 w_d^2 + 2)}{4w_c^2 w_d^2 - 1} \sin 2\psi_0 + (w_d^2 + 3) \sin 2\psi_1 + \\
& \frac{3w_d^2 + 1}{2w_d} \sin 2\pi \frac{w_d}{w_c}] - \frac{3}{4w_c^2 w_d^2 - 1} [(4w_d^2 - 1) \sin 2\psi_1 \cos 2\pi \frac{w_d}{w_c} + w_d(2w_d^2 + 1) \\
& \cos 2\psi_1 \sin 2\pi \frac{w_d}{w_c}] + (2 + 2n - n^2)(w_c^2 - 1)[2(w_c^2 - 1) \frac{\pi}{w_c^3} - \frac{4w_d^2(w_c^2 - 1)}{4w_c^2 w_d^2 - 1} \sin 2\psi_0 \\
& + \sin 2\psi_1 - \frac{1}{2w_d} \sin 2\pi \frac{w_d}{w_c} - \frac{1}{4w_c^2 w_d^2 - 1} [(4w_d^2 - 1) \sin 2\psi_1 \cos 2\pi \frac{w_d}{w_c} + w_d \\
& (2w_d^2 + 1) \cos 2\psi_1 \sin 2\pi \frac{w_d}{w_c}]]] \quad (2.68)
\end{aligned}$$

$$\begin{aligned}
\frac{D_{03}}{d} = & \frac{w_c^2 - 1}{32w_d^4 \sin^4 \psi_0} [-\frac{1}{3} [2(2 + n)w_d(1 - \cos 2\psi_1)(1 - \cos 2\pi \frac{w_d}{w_c}) \sin 2\pi \frac{w_d}{w_c} + (4 - n) \\
& (\cos 4\pi \frac{w_d}{w_c} - 4 \cos 2\pi \frac{w_d}{w_c} + 3) \sin 2\psi_1] - (w_d^2 + 3) \frac{\pi}{w_c} + \frac{2w_d^4(5 + w_c^2)}{(w_c^2 - 1)(4w_d^2 - 1)} \sin 2\psi_0 \\
& + \frac{1 + w_c^2}{2} \sin 2\psi_1 + \frac{2}{w_d} \sin 2\pi \frac{w_d}{w_c} - \frac{w_c^2 - 1}{4w_d} \sin 4\pi \frac{w_d}{w_c} - \frac{2}{w_c^2 - 1} [(w_d^2 + 1) \sin 2\psi_1 \\
& \cos 2\pi \frac{w_d}{w_c} + 2w_d \cos 2\psi_1 \sin 2\pi \frac{w_d}{w_c}] - \frac{1}{2(4w_d^2 - 1)} [(5w_d^2 + 1) \sin 2\psi_1 \cos 4\pi \frac{w_d}{w_c} + \\
& 2w_d(w_d^2 + 2) \cos 2\psi_1 \sin 4\pi \frac{w_d}{w_c}] + \frac{1}{3} (2 - 2n + 3n^2)(w_c^2 - 1) [\frac{3\pi}{w_c} + \frac{6w_d^4}{(w_c^2 - 1)(4w_d^2 - 1)} \\
& \sin 2\psi_0 + \frac{3}{2} \sin 2\psi_1 - \frac{2}{w_d} \sin 2\pi \frac{w_d}{w_c} + \frac{1}{4w_d} \sin 4\pi \frac{w_d}{w_c} - \frac{2}{w_c^2 - 1} (\sin 2\psi_1 \cos 2\pi \frac{w_d}{w_c} + \\
& w_d \cos 2\psi_1 \sin 2\pi \frac{w_d}{w_c}) - \frac{1}{2(4w_d^2 - 1)} (\sin 2\psi_1 \cos 4\pi \frac{w_d}{w_c} + 2w_d \cos 2\psi_1 \sin 4\pi \frac{w_d}{w_c}]] \quad (2.69)
\end{aligned}$$

$$\frac{D_{21}}{d} = \frac{C_{12}}{d} - \frac{1}{8w_d^2 \sin^4 \psi_0} [(1 - \cos 2\pi \frac{w_d}{w_c}) \sin 2\psi_1 + w_d(1 - \cos 2\psi_1) \sin 2\pi \frac{w_d}{w_c}] \quad (2.70)$$

where $\psi_0 = a \cot\left(\frac{z_0}{d}\right)$ and $\psi_1 = a \cot\left(\frac{z_1}{d}\right)$

ψ_0 corresponds to the position of the object and ψ_1 to that of the image.

2-4 Computer Program for Computing The Beam Trajectory, The Optical Properties and Aberration Coefficients of Combined Quadrupole Lens

A computer program with MathCAD professional 2001i has been used for determining the trajectory of charged particles traversing the field of combined quadrupole lens in both the convergence plane and divergence plane, by using the transfer matrices given in equations (2.14) to (2.15) and (2.46) to (2.47) where the axial potential field has been compute to have a field model which close to its distribution. The first order optical properties such as the focal length and magnification have been computed with the aid of equations (2.31) to (2.35) and (2.51) to (2.52) in the planes of convergence and divergence. The chromatic aberration coefficients C_{cx} , C_{cy} , C_{mx} , and C_{my} and spherical aberration coefficients C_{30} , C_{12} , D_{03} , and D_{21} are computing by using equations (2.55) to (2.68) for each design of combined quadrupole lens. Figure (2-3) illustrates a block diagram of this computer program.

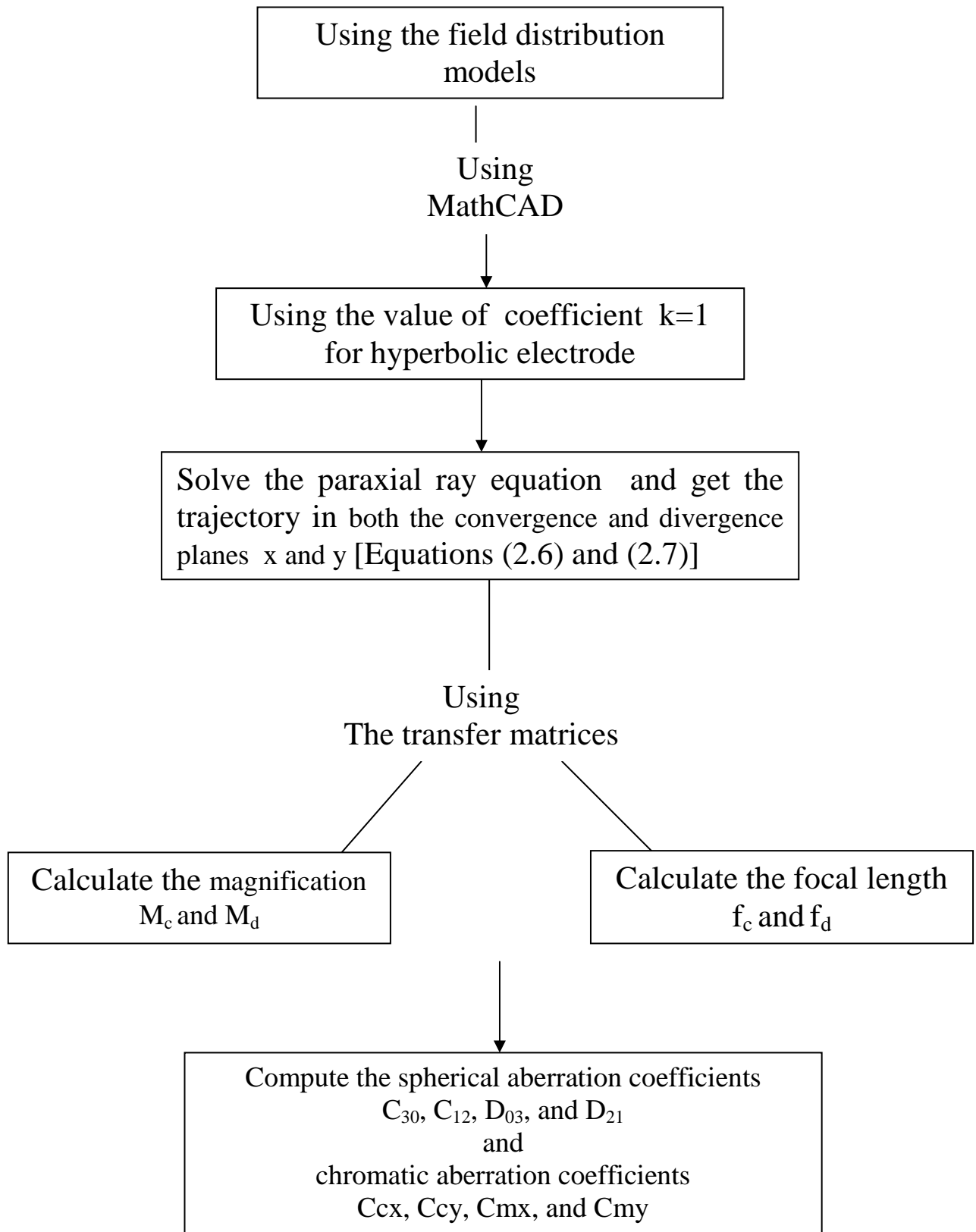


Figure (2-3): A block diagram of the MathCAD program for computing, the axial potential distribution, the trajectory, the optical properties and the aberration coefficients of electrostatic quadrupole lens.

3- RESULTS AND DISCUSSION

3-1 Introduction

The purpose of present work is finding the optimum properties of combined quadrupole lens consists of electrostatic and magnetic lenses to produce achromatic lens. Two models of potential, rectangular model and bell-shaped model, are used to find the optimum design of the lens. The optimization is made in each model by solving the equation of motion and finding the transfer matrices in convergence and divergence planes. Which are used to find the properties of lens as focal length, magnification and aberrations coefficients, taking into account electrode shape in two models is hyperbolic cross section ($k = 1$). To find the optimum values of chromatic and spherical aberrations coefficients. The effects of changing the effective length of lens "L"(geometrical dimensions) and excitation of lens with changing object and image distances.

3-2 Rectangular Model

3-2-1 Trajectory equation of motion of charge particles for the combined quadrupole lens

The trajectory equation of charge particles has been solved for the rectangular model case by using simplified transformation for equations [(2.6) and (2.7)]. These equations describe the paths of charge particles in convergence and divergence plane respectively. In combined quadrupole lens (electrostatic and magnetic) charge particles incident in the (x-z) plane different paths from that in the (y-z) plane the describe in figure (3-1). The charge particles in the convergence plane (x-z) in the figure deflected toward the optical axis and away from the optical axis in the divergence plane (y-z).

i.e. the combined quadrupole lens is astigmatic, and the results is coincide with that published by Baranova and Yavor [1984] and agreement the speech is trajectories to be parallel to the optical axis and to lie to the left and to the right of the lens, respectively. when taked value excitation lens ($\beta(\text{mm}^{-1})$) equal to (0.1mm^{-1}) and (z) value about range from (zero) to (10mm) with choose best initial condition for gets on trajectory for charge particles in case rectangular model.

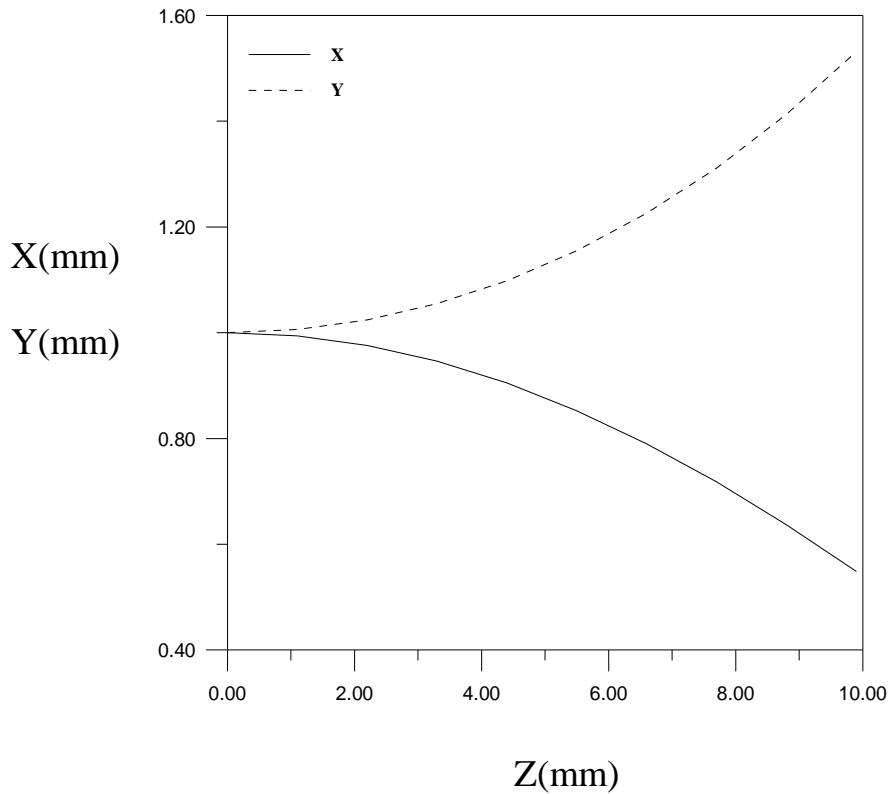


Figure (3-1): Trajectory of charge particles in combined quadrupole lens for both convergence (x-z) plane and divergence (y-z) plane.

3-2-2 Optical properties for the combined quadrupole lens

After solving trajectory equations and finding the transfer matrices (T_c and T_d), in the convergence and divergence planes, the matrix elements are used to calculate both focal length and magnification. The calculation of optimization are made for two values of effective length of lens, ($L_1= 0.9\text{mm}$ and $L_2= 1\text{mm}$), to study the effect of effective length of the lens on its properties.

3-2-2-1 focal length

The calculation of focal length for two values of effective length of lens $L_1= 0.9\text{mm}$ and $L_2=1\text{mm}$ are shown in figures (3-2) and (3-3) for convergence and divergence planes, respectively.

Figure (3-2) shows the relation between the focal length and $(\theta=\beta L)$ for the convergence case. From the figure the focal length decreases as θ increases. The calculations show that the effective length $L_2(1\text{mm})$ has focal length values greater than that of effective length $L_1(0.9\text{mm})$.

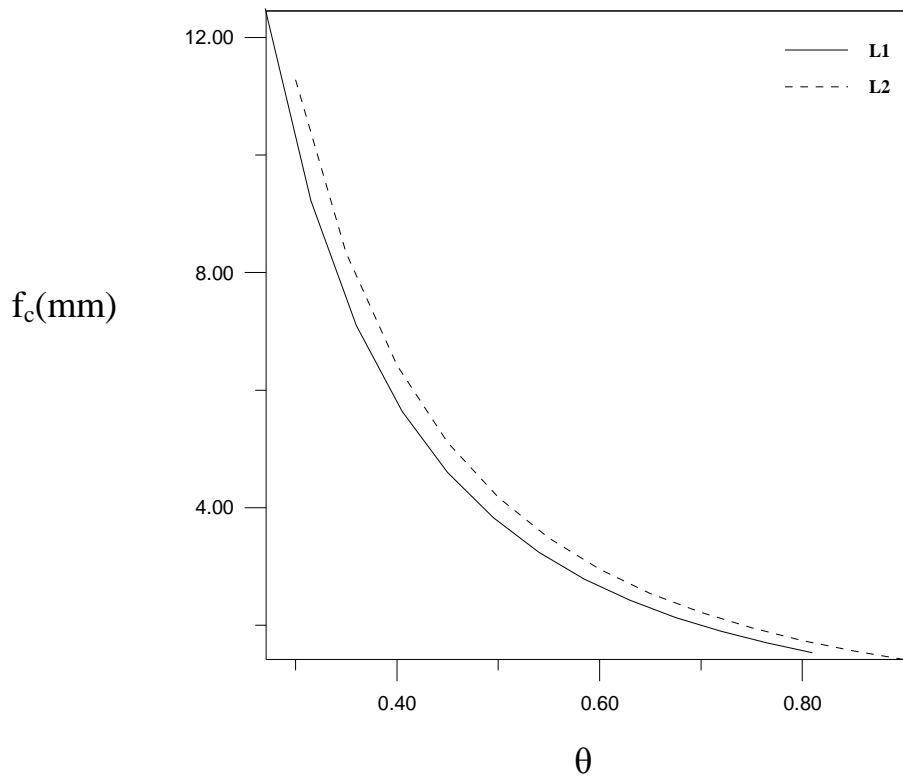


Figure (3-2): The focal length as a function of θ for the combined quadrupole lens in convergence plane for the effective lengths of lens $L1=0.9\text{mm}$ and $L2=1\text{mm}$.

The focal length calculations in divergence plane is shown in figure (3-3) opposite behaviour to the case of convergence plane, where the focal length increases with the increasing of the values of θ . From the figure, the effective length $L1(0.9\text{mm})$ has values of focal length greater than that of effective length $L2(1\text{mm})$.

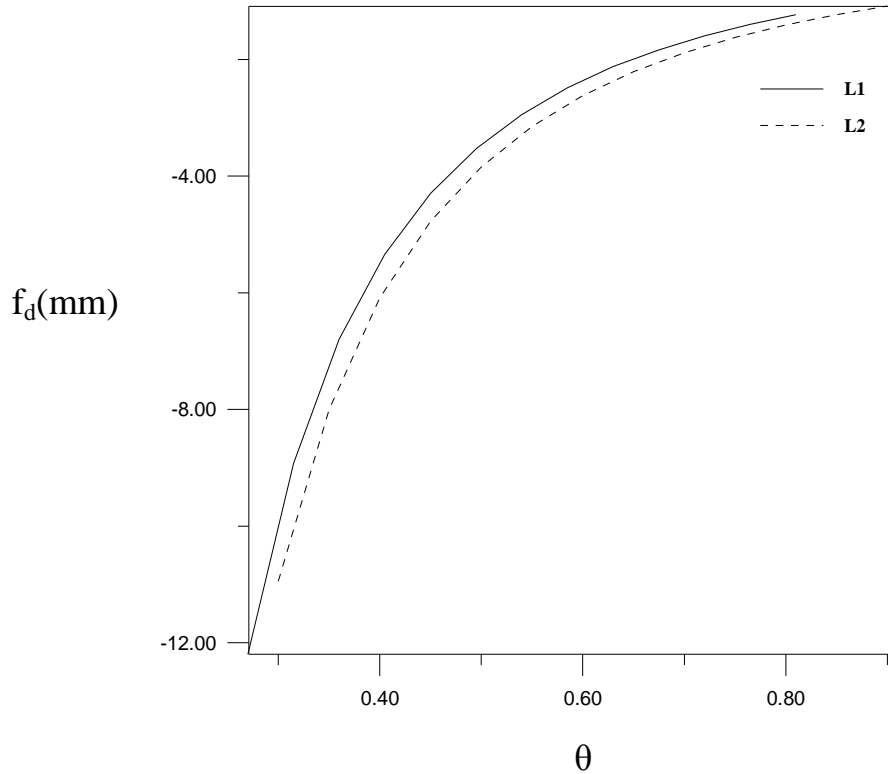


Figure (3-3): The focal length as a function of θ for the combined quadrupole lens in divergence plane for the effective lengths of lens $L1=0.9\text{mm}$ and $L2=1\text{mm}$.

The relations between the focal length and relative excitation parameter (n) ($n = \beta e^2 / \beta^2$) for convergence and divergence planes are shown in figures (3-4) and (3-5), respectively.

From figure (3-4) the focal length of the convergence case is increases with increasing the values of relative excitation parameter (n). The effective length $L1(0.9\text{mm})$ has the values of focal length greater than that of $L2(1\text{mm})$.

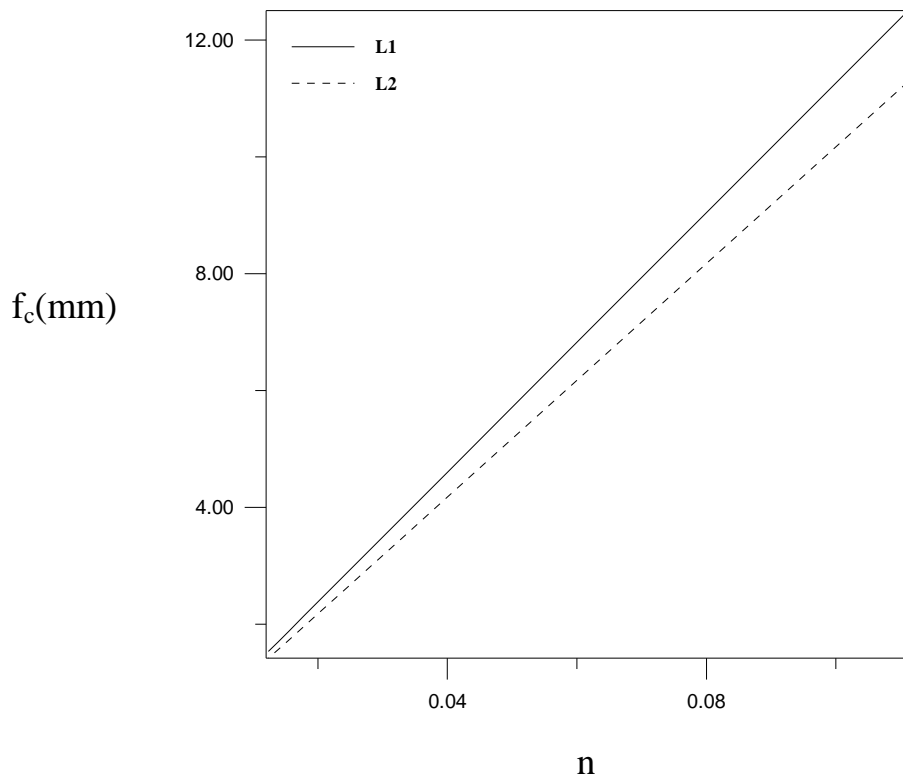


Figure (3-4): The focal length as a function of relative excitation parameter (n) for the combined quadrupole lens in the convergence plane for the two effective lengths of lens $L1=0.9\text{mm}$ and $L2=1\text{mm}$.

The calculations of the divergence case are shown in figure (3-5). The results shown appear an opposite behaviour to that in the convergence case, where the focal length decreases as increasing n and the effective length $L2(1\text{mm})$ has values of focal length greater than that of $L1(0.9\text{mm})$.

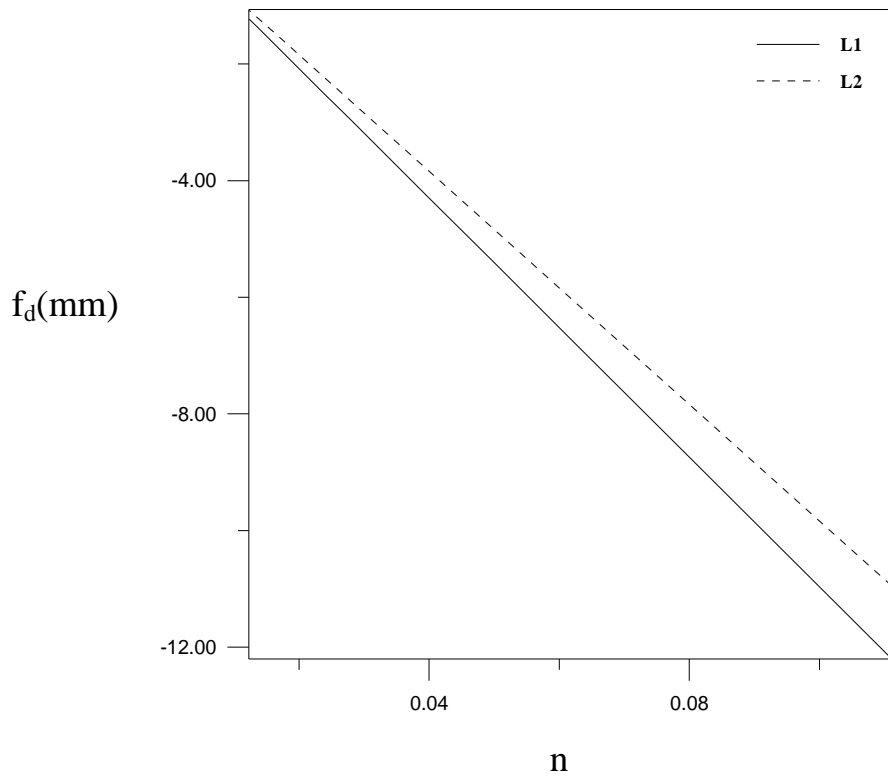


Figure (3-5): The focal length as a function of relative excitation parameter (n) for the combined quadrupole lens in the divergence plane for the two effective lengths $L1=0.9\text{mm}$ and $L2=1\text{mm}$

3-2-2-2 magnification

The effect of changing the effective length of lens on the magnification for both convergence and divergence planes are shown in figures (3-6) and (3-7), respectively. Figure (3-6), shows the relation between magnification and θ in the convergence plane. The magnification increases with increasing θ values and the values of magnification for both effective lengths $L1(0.9\text{mm})$ and $L2(1\text{mm})$ are closer to each other.

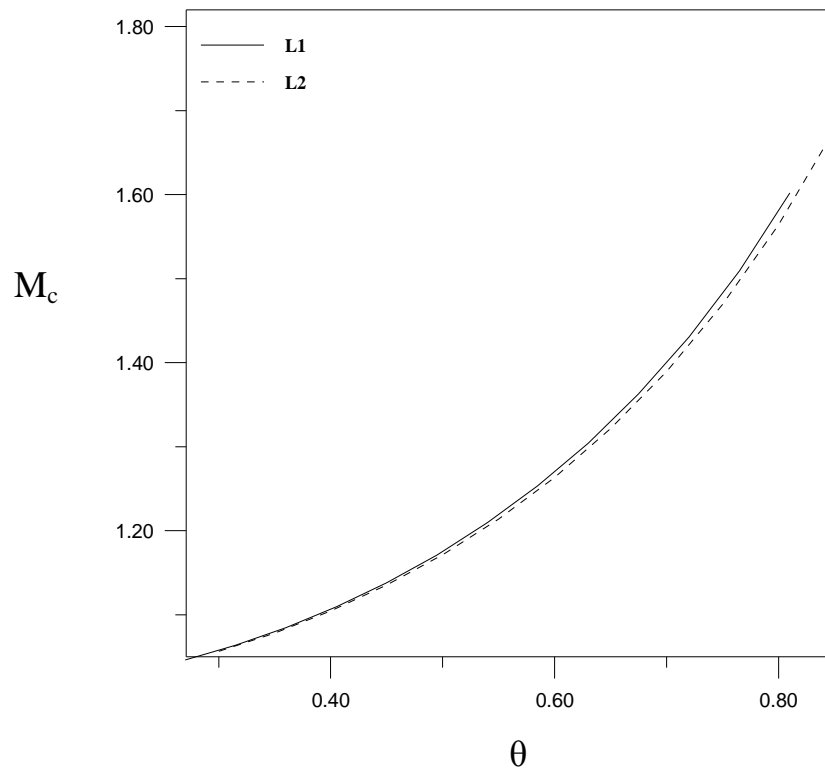


Figure (3-6): The magnification as a function of θ for the combined quadrupole lens in convergence plane for the effective lengths of lens $L1=0.9\text{mm}$ and $L2=1\text{mm}$.

The behaviour of magnification for divergence plane is opposite to that of convergence plane as is shown in figure (3-7), where the magnification decreases as the values of θ increase. Also, both effective lengths $L1(0.9\text{mm})$ and $L2(1\text{mm})$ have closer values of magnification.

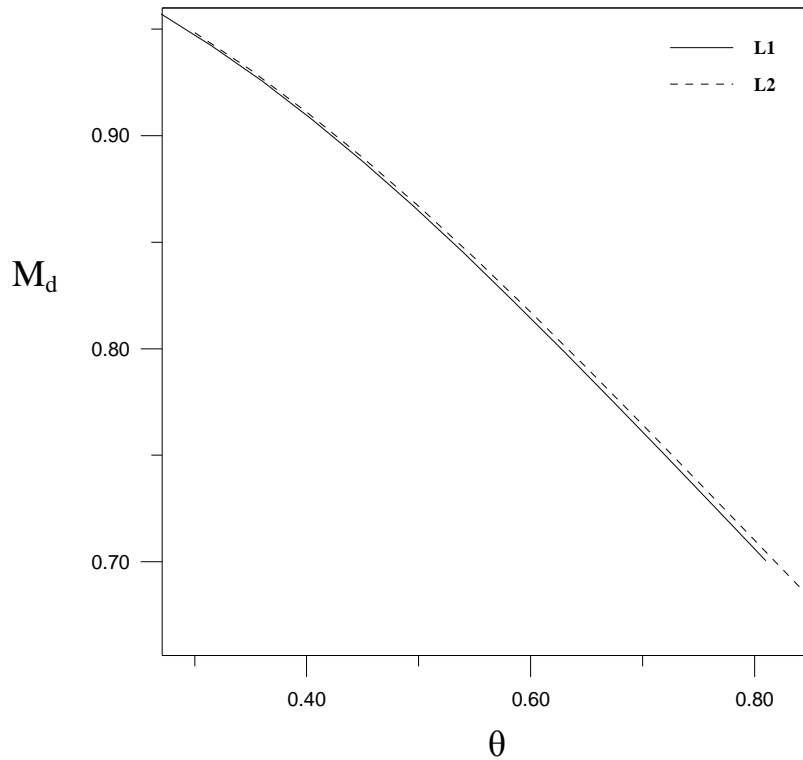


Figure (3-7): The magnification as a function of θ for the combined quadrupole lens in divergence plane for the effective lengths of lens $L1=0.9\text{mm}$ and $L2=1\text{mm}$.

The relation between the magnification and relative excitation parameter (n) is shown for both convergence and divergence plane in figures (3-8) and (3-9), respectively.

In the case of convergence plane, the magnification decreases as the relative excitation parameter (n) increases and the effective length of lens L1 has the values of magnification lower than that of L2. while the opposite magnification behaviour is found for the case of divergence case.

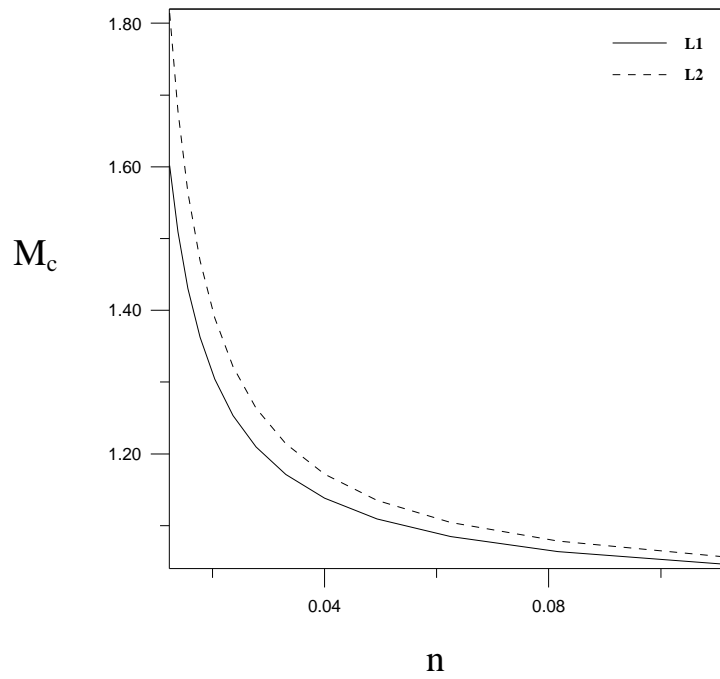


Figure (3-8): The magnification as a function of relative excitation parameter (n) for the combined quadrupole lens in convergence plane for the effective lengths of lens $L1=0.9\text{mm}$ and $L2=1\text{mm}$.

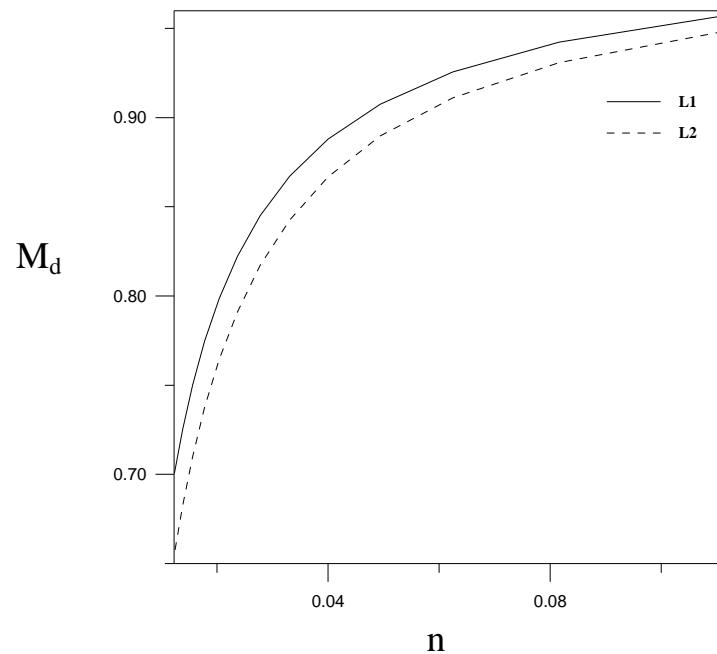


Figure (3-9): The magnification as a function of relative excitation parameter (n) for the combined quadrupole lens in divergence plane for the effective lengths of lens $L1=0.9\text{mm}$ and $L2=1\text{mm}$.

3-2-3 The chromatic and spherical aberrations for the combined quadrupole lens

3-2-3-1 the chromatic aberration

The optimization calculations for chromatic aberration coefficients in both convergence and divergence plane are made for two values of effective length of lens, ($L_1 = 0.9\text{mm}$ and $L_2 = 1\text{mm}$) to produce achromatic lens.

In figures (3-10) and (3-11) the results of chromatic aberration coefficients are shown for convergence plane, respectively. The figure (3-10) shows the relation between chromatic aberration coefficient C_{cx}/L with θ . We find from the figure the chromatic aberration coefficient C_{cx}/L decreases (take always negative) as θ increases. The sign of the chromatic aberration coefficients can change for systems composed of both electrostatic and magnetic quadrupole lenses. The simplest example is the achromatic lens obtained by superposing electric and magnetic quadrupole fields and satisfy the formulae by Baranova and Yavor [1984].

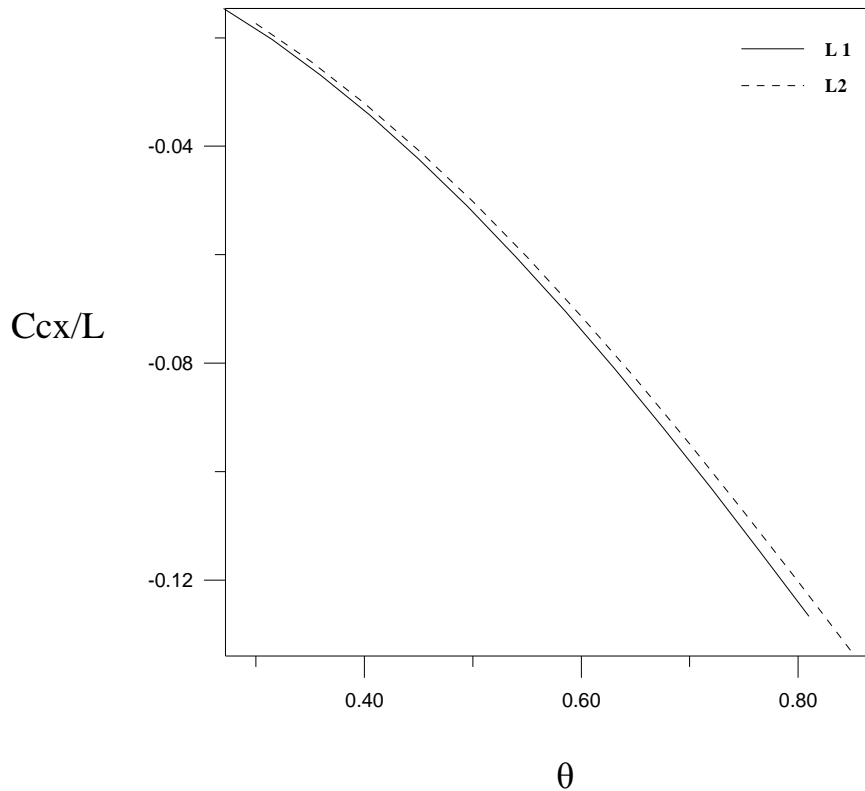


Figure (3-10): The relative chromatic aberration coefficients as a function of θ for the combined quadrupole lens in convergence plane for two effective lengths of lens $L1=0.9\text{mm}$ and $L2=1\text{mm}$.

The calculations of chromatic aberration coefficient change of magnification C_{mx} are shown in figure (3-11) and the results shows appear the same behaviour to the chromatic aberration coefficient C_{cx}/L , but with greater values than that of chromatic aberration coefficient C_{cx}/L and decrease as θ is increasing.

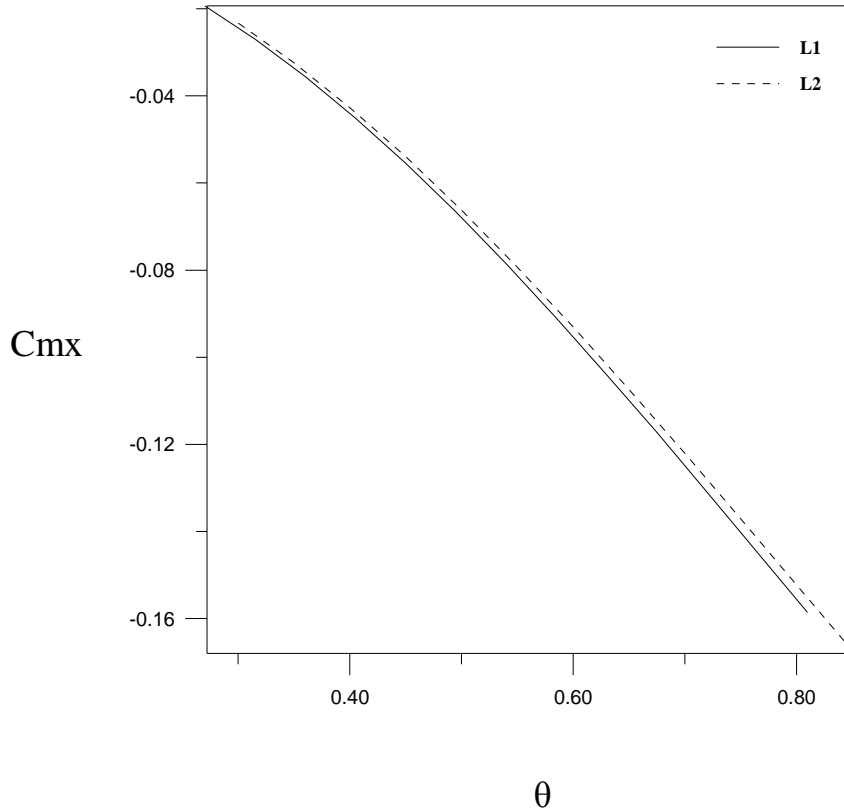
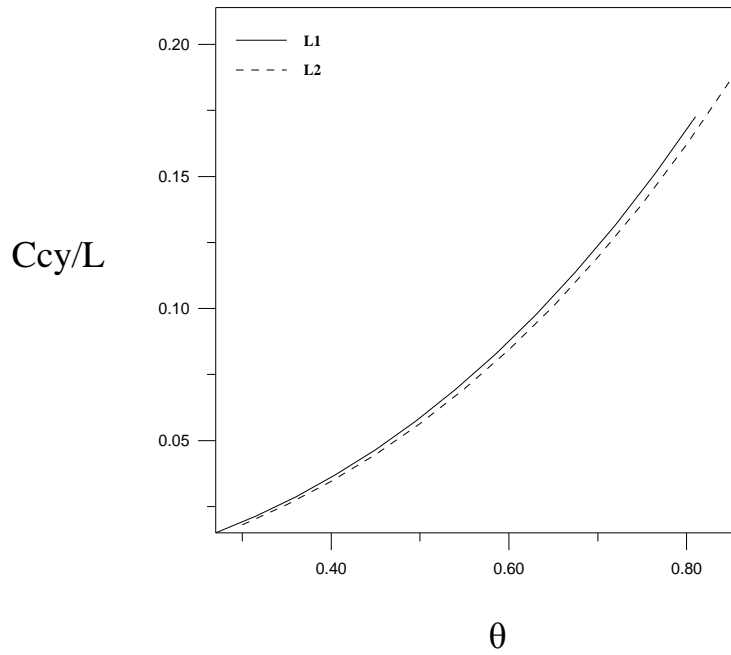


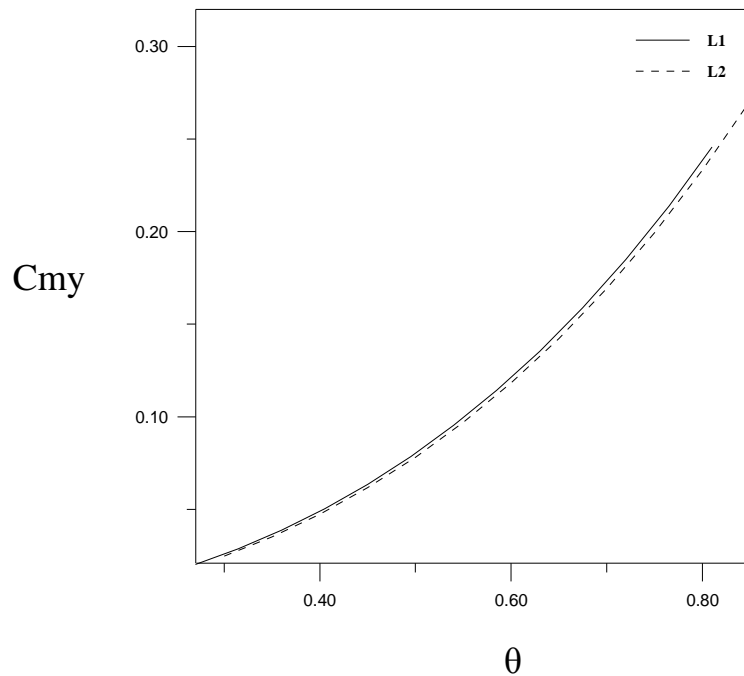
Figure (3-11): The relative chromatic aberration coefficients change of magnification as a function of θ for the combined quadrupole lens in convergence plane for the effective lengths of lens $L1=0.9\text{mm}$ and $L2=1\text{mm}$.

The calculations of chromatic aberration coefficients C_{cy}/L and C_{my} for the divergence case are shown in figures (3-12) and (3-13) respectively.

Figure (3-12) shows the relation between chromatic aberration coefficient C_{cy}/L and θ . From the figure one can see a different behaviour for the convergence case (chromatic aberration coefficients C_{cx}/L and C_{mx}), where the chromatic aberration coefficient C_{cy}/L increase as θ increasing. The effective lengths of lens at $L1$ (0.9mm) and $L2$ (1mm) have the values closer to each other. From figure (3-13) the chromatic aberration coefficient change of magnification C_{my} has the same behaviour to that of C_{cy}/L .



Figure(3-12): The relative chromatic aberration coefficients as a function of θ for the combined quadrupole lens in divergence plane for the effective lengths of lens $L1=0.9\text{mm}$ and $L2=1\text{mm}$.



Figure(3-13): The relative chromatic aberration coefficients change of magnification as a function of θ for the combined quadrupole lens in divergence plane for the effective lengths of lens $L1=0.9\text{mm}$ and $L2=1\text{mm}$.

From the calculations in both convergence and divergence planes, the calculations shows that the best effective length of lens is L1(0.9mm) and the chromatic aberration coefficients can be reduced by using a combined electrostatic and magnetic quadrupole lenses and obtained an achromatic case which is similar to that which is given by Baranove and Read [1999]. The calculations which in obtained on it is best than that result which is investigation by Martin and Goloskie [1982].

The plote between the chromatic aberration coefficient and relative excitation parameter (n) is shown for both convergence and divergence planes in the figures (3-14) to (3-17), respectively. The chromatic aberration coefficient C_{cx}/L increases as the relative excitation parameter (n) increases and the effective length of lens L1 has values of chromatic aberration coefficient C_{cx}/L greater than that of L2 as is shown in figure (3-14).

The same behaviour is found for the calculations of chromatic aberration coefficient change of magnification C_{mx} as is shown in figure (3-15)

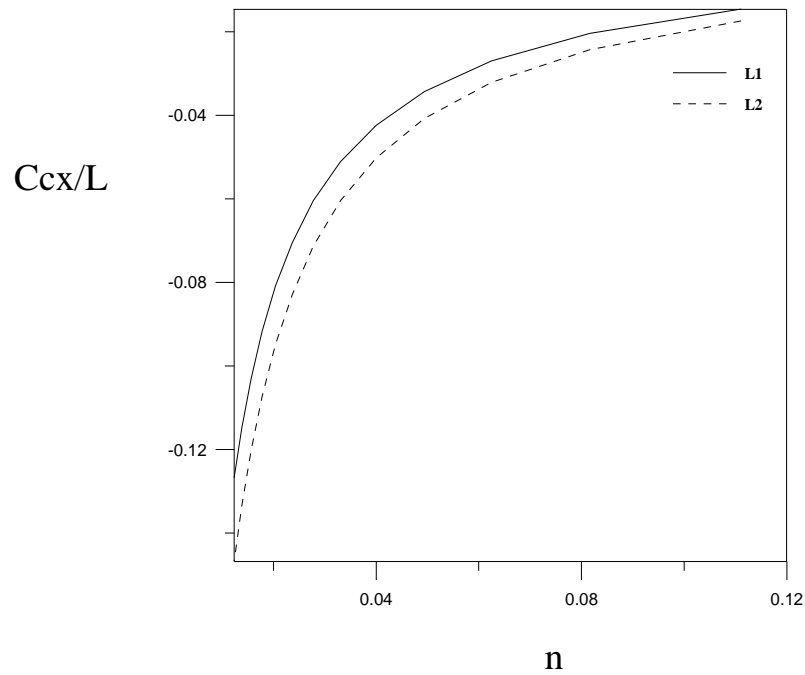


Figure (3-14): The relative chromatic aberration coefficients as a function of relative excitation parameter (n) for the combined quadrupole lens in convergence plane for the effective lengths of lens $L1=0.9\text{mm}$ and $L2=1\text{mm}$.

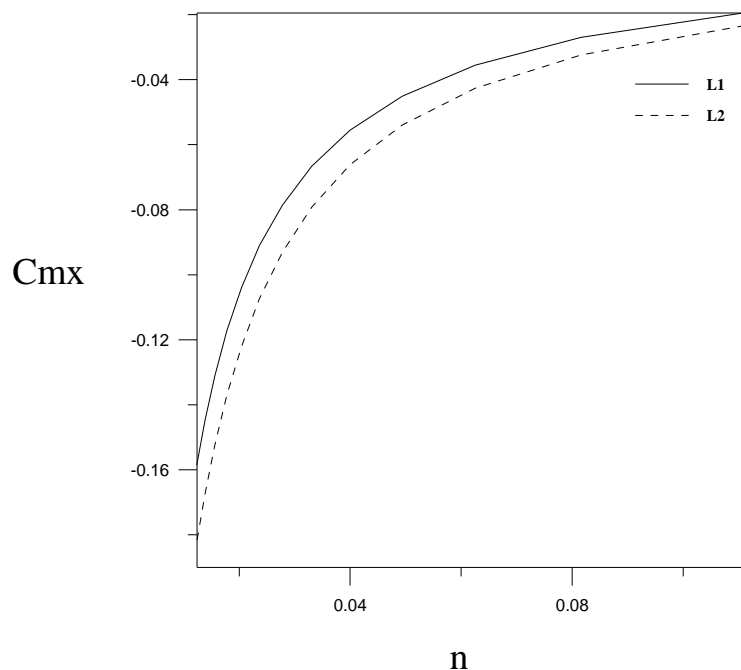


Figure (3-15): The relative chromatic aberration coefficients change of magnification as a function of relative excitation parameter (n) for the combined quadrupole lens in convergence plane for the effective lengths of lens $L1=0.9\text{mm}$ and $L2=1\text{mm}$.

In case of divergence plane the results are shown in figures (3-16) and (3-17). Figure (3-16) appears the results of chromatic aberration coefficient C_{cy}/L which decrease as the relative excitation parameter (n) is increasing and the values of the effective length of lens L1(0.9mm) are lower than that of L2(1mm). The same behaviour of chromatic aberration coefficient change of magnification C_{my} is found as shown in figure (3-17).

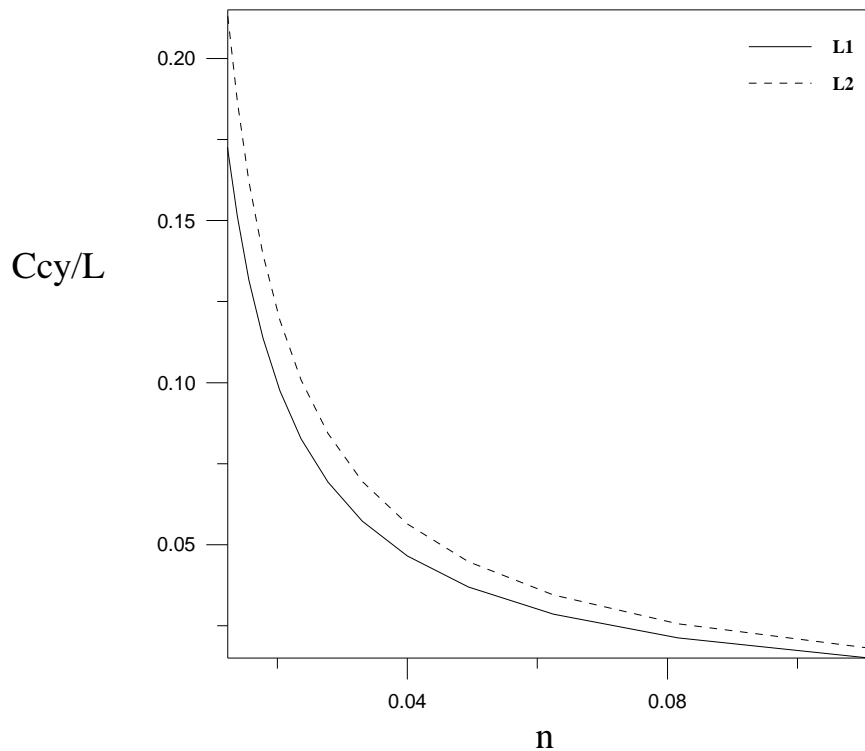


Figure (3-16): The relative chromatic aberration coefficients as a function of relative excitation parameter (n) for the combined quadrupole lens in divergence plane for the effective lengths of lens L1=0.9mm and L2=1mm.

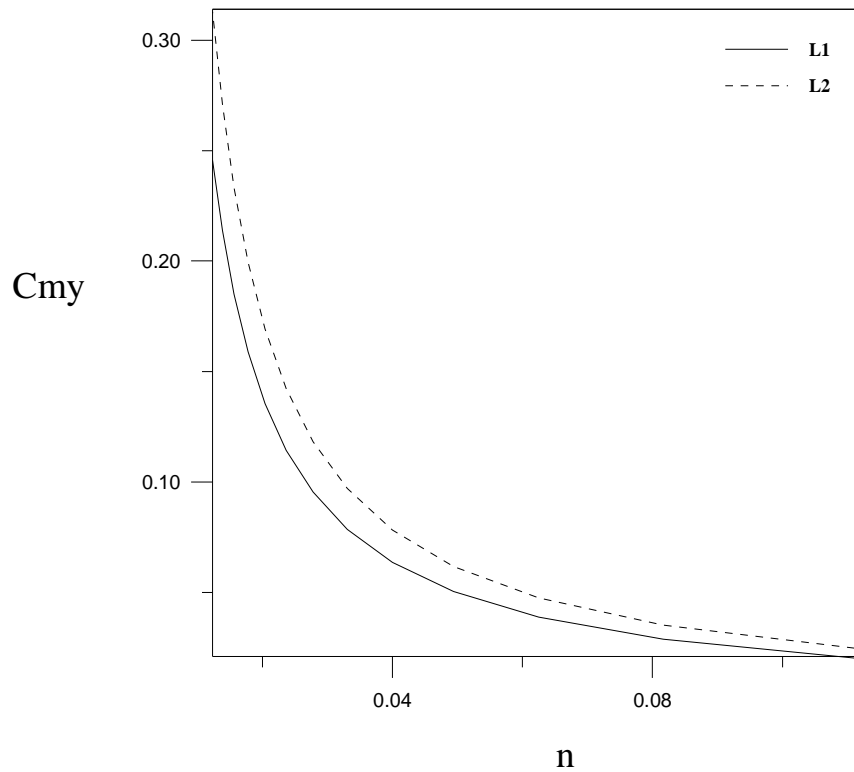


Figure (3-17): The relative chromatic aberration coefficients change of magnification as a function of relative excitation parameter (n) for the combined quadrupole lens in divergence plane for the effective lengths of lens $L1=0.9\text{mm}$ and $L2=1\text{mm}$.

3-2-3-2 the spherical aberration

The optimization calculations for spherical aberration coefficients in both convergence and divergence plane are made to show the effect of changing the excitation parameter and the effective lengths of lens on the spherical aberration coefficients. The calculations of the case of convergence plane are shown in figures (3-18) and (3-19), respectively. Figure (3-18) shows the proportionally relation between spherical aberration coefficient C_{30}/L and θ for the convergence case, where the spherical aberration coefficient C_{30}/L increases as θ is increasing.

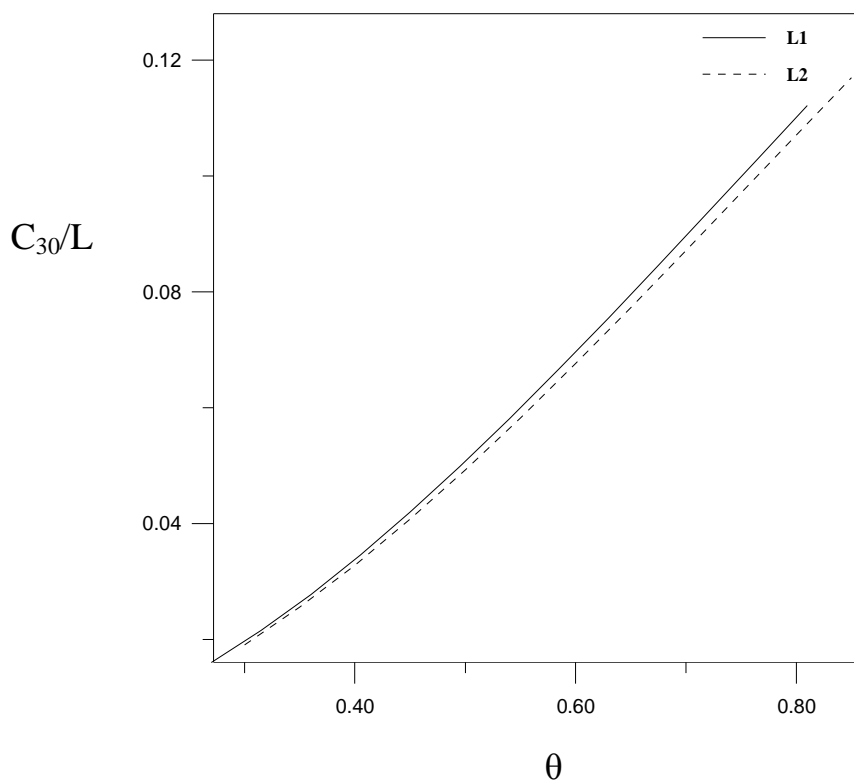


Figure (3-18): The relative spherical aberration coefficients C_{30}/L as a function of θ for the combined quadrupole lens in the convergence plane for two effective lengths of lens $L1=0.9\text{mm}$ and $L2=1\text{mm}$.

The results of spherical aberration coefficient C_{12}/L are shown in figure (3-19). The calculations shows that the values of spherical aberration coefficient C_{12}/L has a minimum value (-0.0046) at θ (0.405) at L1(0.9mm) and L2(1mm) has the minimum value (-0.0057) at θ (0.4) and of spherical aberration coefficient C_{12}/L will be increasing at θ increases.

In the region where $\theta = 0.28$ to 0.5 the results show the zero and negative spherical aberration coefficient values, therefore, the designer can use this operation condition and geometrical dimensions to design the lens with best properties of spherical aberration coefficient. This results are similar to the results published by Dymnikov et al [1965] where the negative and positive values are at the same θ are found but the present results are the best to give rise to minimum spherical aberration coefficient.

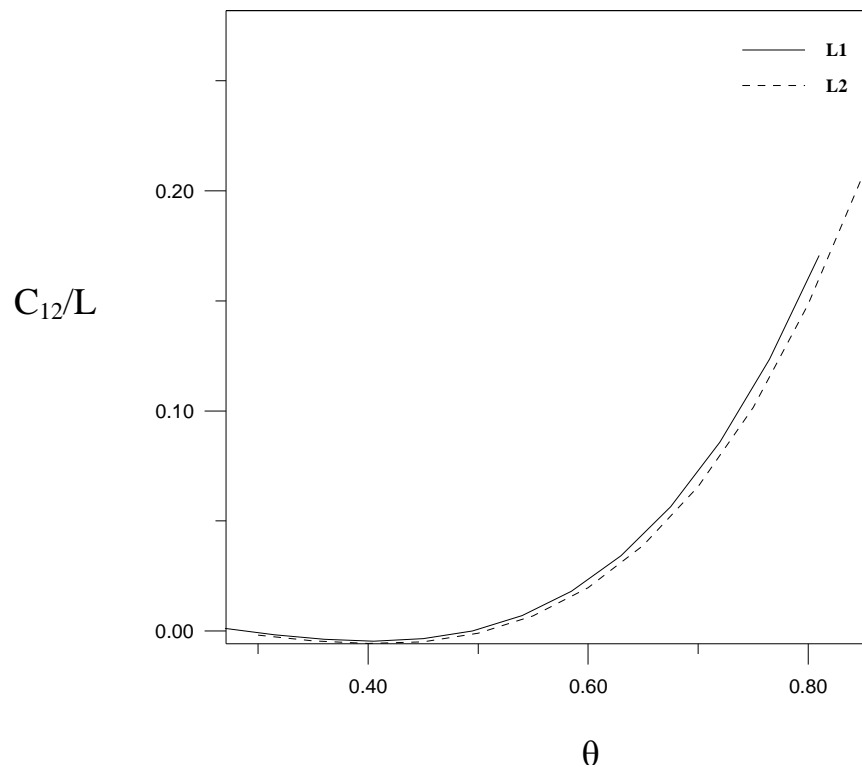


Figure (3-19): The relative spherical aberration coefficients C_{12}/L as a function of θ for the combined quadrupole lens in convergence plane for the effective lengths of lens L1=0.9mm and L2=1mm.

In the case of divergence plane the results are shown in figures (3-20) and (3-21) of the relative coefficients D_{03}/L and D_{21}/L , respectively. The relation between the spherical aberration coefficient D_{03}/L and θ is shown in figure (3-20). From the calculations the spherical aberration coefficient D_{03}/L (take always negative values) become less as θ is increasing. The effective length for lens L2(1mm) has the values slightly greater than that of L1(0.9mm). The present calculations are better than that which were obtained for spherical aberration coefficient D_{03}/L by Dymnikov et al [1965] which had the same behaviour but with values positive and negative at same range of θ but the present values are best than that of Dymnikov et al [1965].

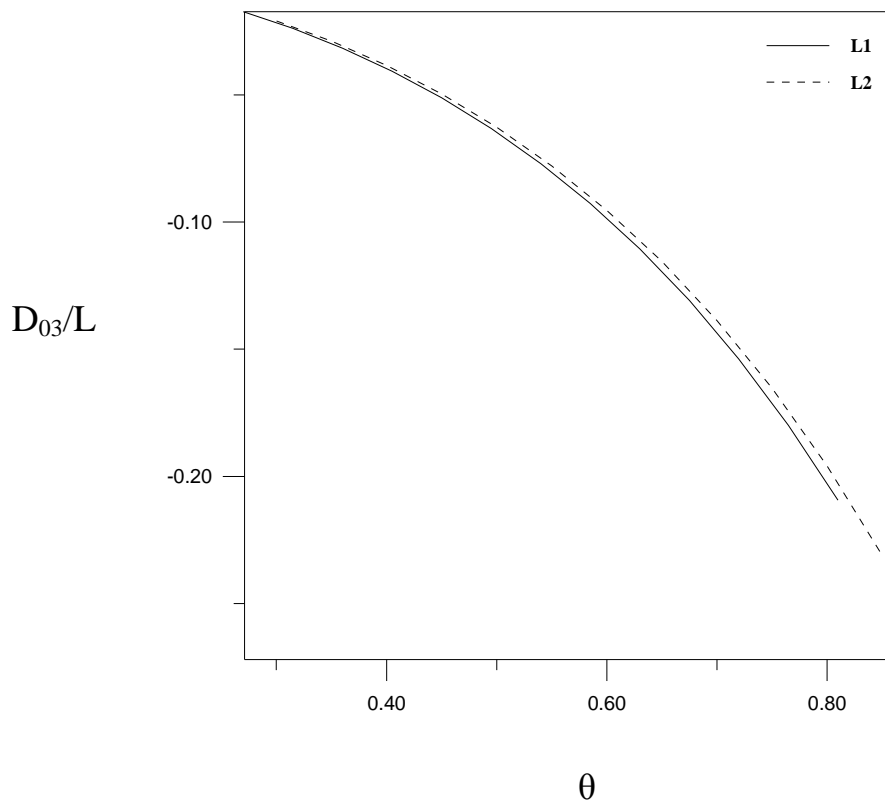
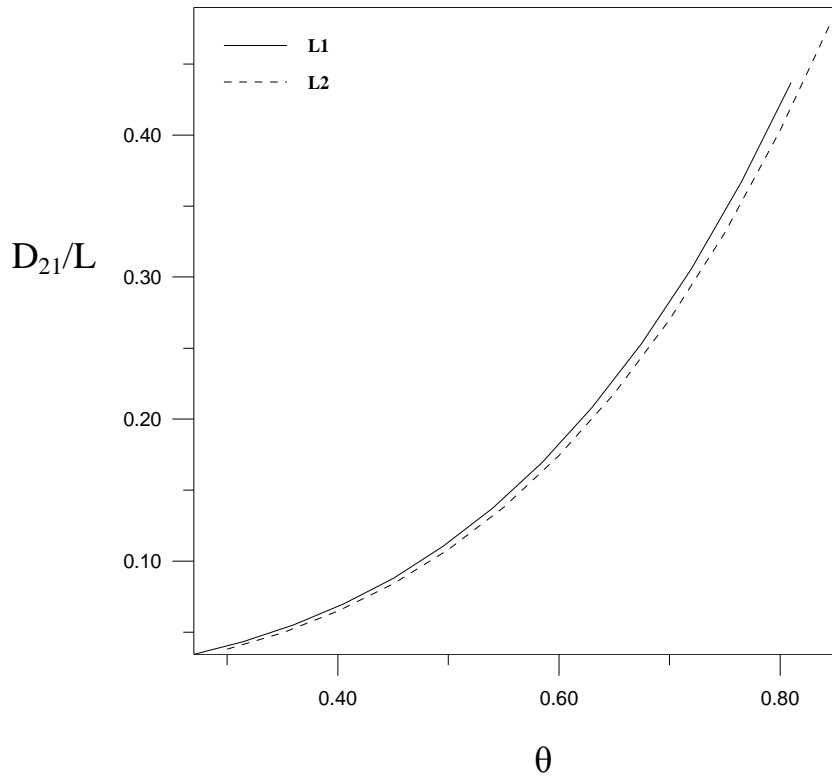


Figure (3-20): The relative spherical aberration coefficients D_{03}/L as a function of θ for the combined quadrupole lens in divergence plane two the effective lengths of lens L1=0.9mm and L2=1mm.

The results appear in the figure (3-21) show the spherical aberration coefficient D_{21}/L increases as θ is increasing, its values for the effective length of lens L1(0.9mm) is greater than that of at L2(1mm).



Figure(3-21): The relative spherical aberration coefficients D_{21}/L as a function of θ for the combined quadrupole lens in divergence plane for two effective lengths of lens L1=0.9mm and L2=1mm.

The relation between spherical aberration coefficients and relative excitation parameter (n) is shown for both convergence and divergence planes in figures (3-22) to (3-25). The figures (3-22) and (3-23), are explain the spherical aberration coefficients as the function of relative excitation parameter (n) for the case convergence plane. In figure (3-22) the spherical aberration coefficient C_{30}/L decrease as n is increasing and the effective length

L1(0.9mm) has the values of spherical aberration coefficient lower than that of L2(1mm).

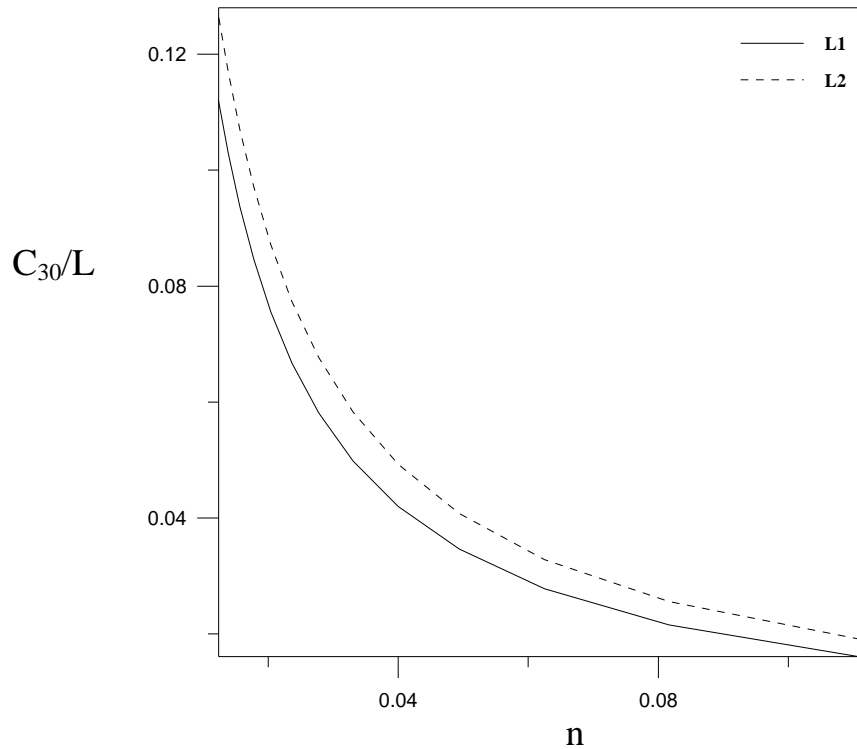


Figure (3-22): The relative spherical aberration coefficients C_{30}/L as a function of relative excitation parameter (n) for the combined quadrupole lens in convergence plane for the effective lengths of lens $L1=0.9\text{mm}$ and $L2=1\text{mm}$.

From figure (3-23) the spherical aberration coefficient C_{12}/L has inverse relation to the relative excitation parameter (n) and the calculations show the slightly difference between two effective lengths of lens and nearly the $n = 0.063$ both effective lengths have minimum spherical aberration coefficient.

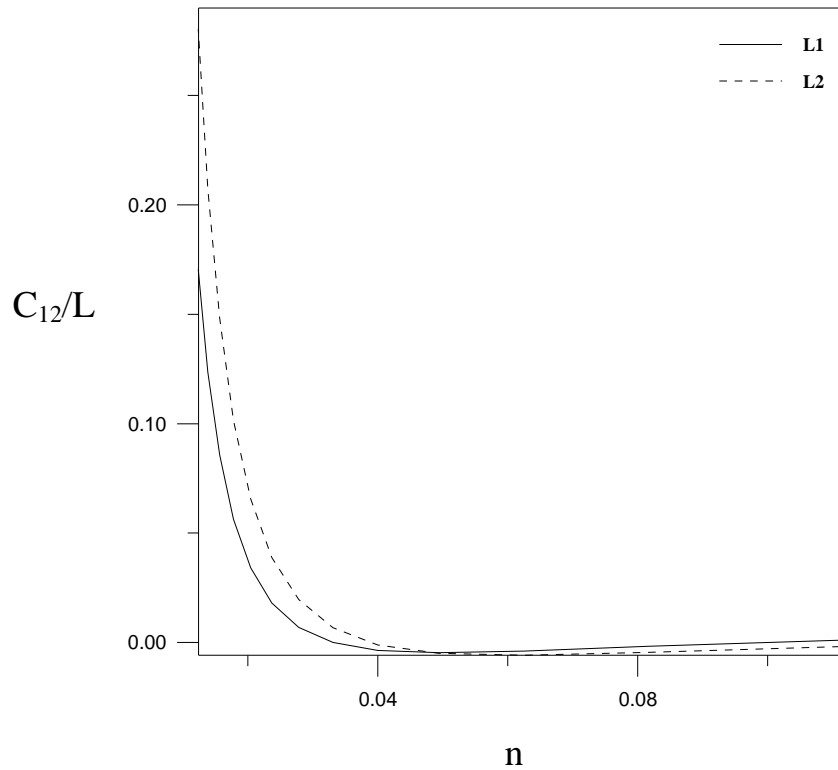
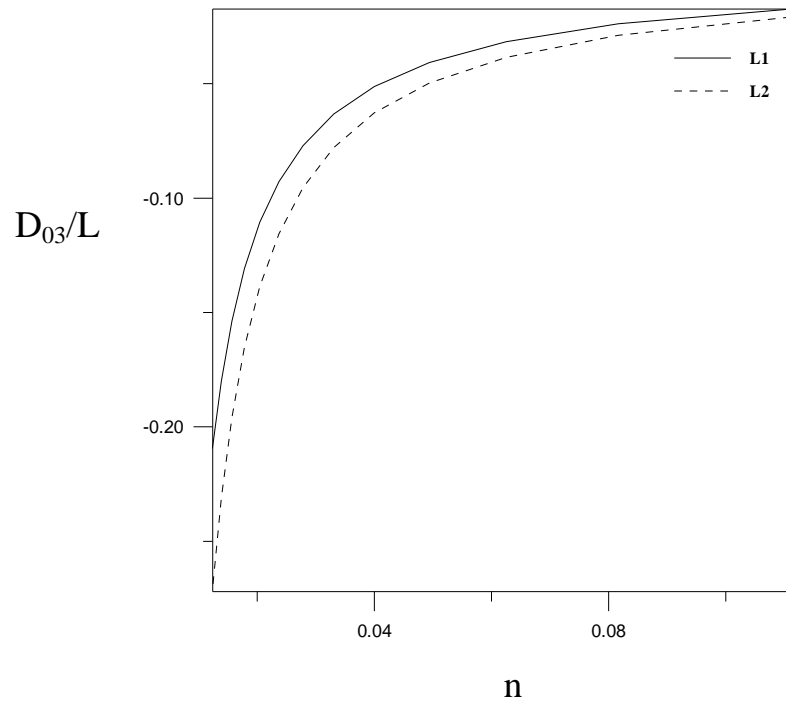


Figure (3-23): The relative spherical aberration coefficients C_{12}/L as a function of relative excitation parameter (n) for the combined quadrupole lens in convergence plane for the effective lengths of lens $L1=0.9\text{mm}$ and $L2=1\text{mm}$.

The calculations of divergence case are shown in figures (3-24) and (3-25). The figure (3-24) the relation between spherical aberration coefficient D_{30}/L and relative excitation parameter (n), this coefficient increases as n increases and the effective length $L2(1\text{mm})$ give us the best result with respect to another effective length $L1(0.9\text{mm})$.

The relation between spherical aberration coefficient D_{21}/L and relative excitation parameter (n) is shown in figure (3-25), this relation is found to be inversely and the effective length of lens $L1$ give us the optimum results with respect to another effective length of lens $L2$.



Figure(3-24): The relative spherical aberration coefficients D_{30}/L as a function of relative excitation parameter (n) for the combined quadrupole lens in divergence plane for the effective lengths of lens $L1=0.9\text{mm}$ and $L2=1\text{mm}$.

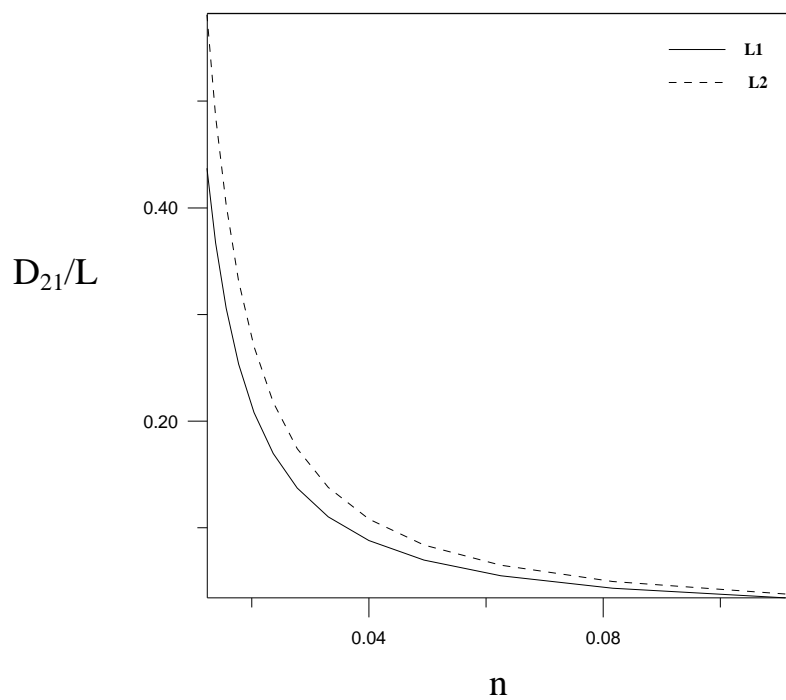


Figure (3-25): The relative spherical aberration coefficients D_{21}/L as a function of relative excitation parameter (n) for the combined quadrupole lens in divergence plane for the effective lengths of lens $L1=0.9\text{mm}$ and $L2=1\text{mm}$.

3-3 Bell-Shaped Model

3-3-1 Trajectory equation of motion of charge particles for the combined quadrupole lens

The trajectory of charged particles beam is computed by using the bell-shaped model for combined quadrupole lens, and the result is shown in figure (3-26). From figure (3-26) we notice the same behaviour for the two cases of convergence and divergence planes for rectangular model, but the case of convergence for bell-shaped model is begin at 1 and the decreasing is slow in compare with the case of rectangular model and opposite behaviour in divergence.

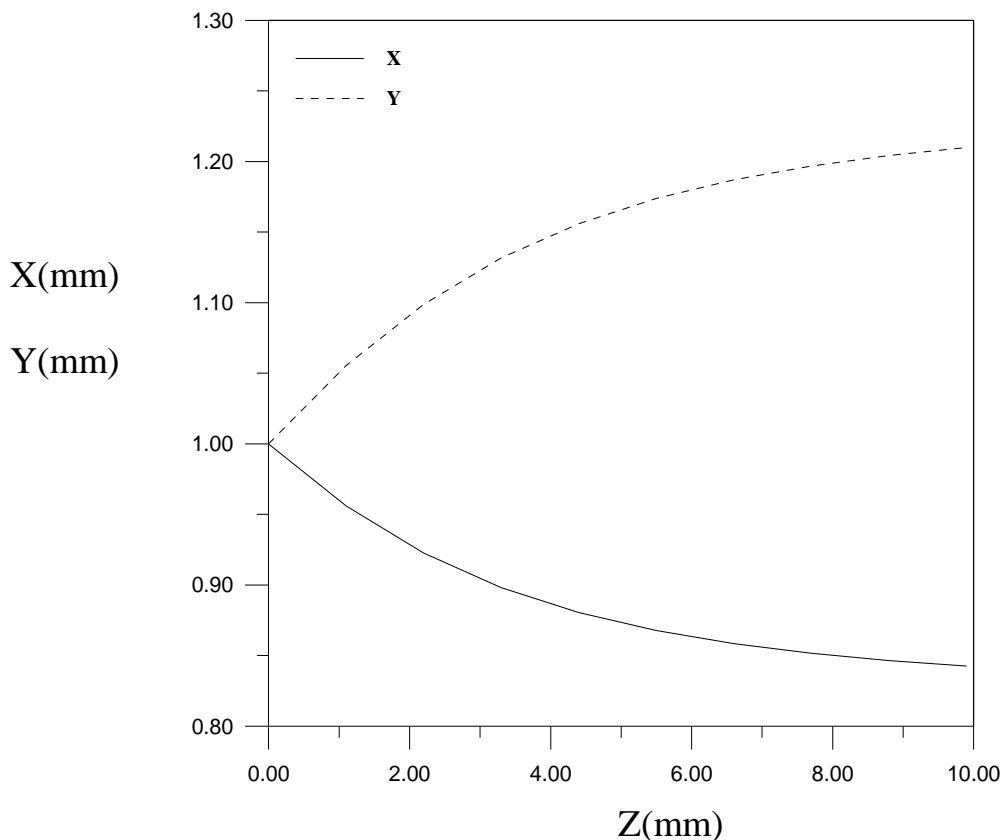


Figure (3-26): Trajectory of charge particles beam in combined quadrupole lens for both convergence (x-z) plane and divergence (y-z) plane.

3-3-2 Optical properties for the combined quadrupole lens

After solving the trajectory equations in both convergence and divergence planes and finding the transfer matrix elements, the focal length and magnification are computed. The effect of effective lengths of lens (L1(0.9mm) and L2(1mm)) is studied on properties of focal length and magnification.

3-3-2-1 focal length

The calculations of focal length in both convergence and divergence planes for two values of effective lengths of lens L1(0.9mm) and L2(1mm) are shown in figures (3-27) and (3-28), respectively.

The figure (3-27) shows the relation between the focal length and $\beta^2 d^2$ for convergence case. From the figure the focal length decreases as increasing $\beta^2 d^2$. The result shows that both the effective lengths L1 and L2 are closer to each other.

The calculations of focal length in divergence plane, is explained in figure (3-28) and the opposite behaviour to the case of convergence plane is found, when the focal length increases with $\beta^2 d^2$ values is increasing. From the figure, the effective length L2(1mm) has values of focal length slightly greater than that of L1(0.9mm) and closer each other, at low values of $\beta^2 d^2$.

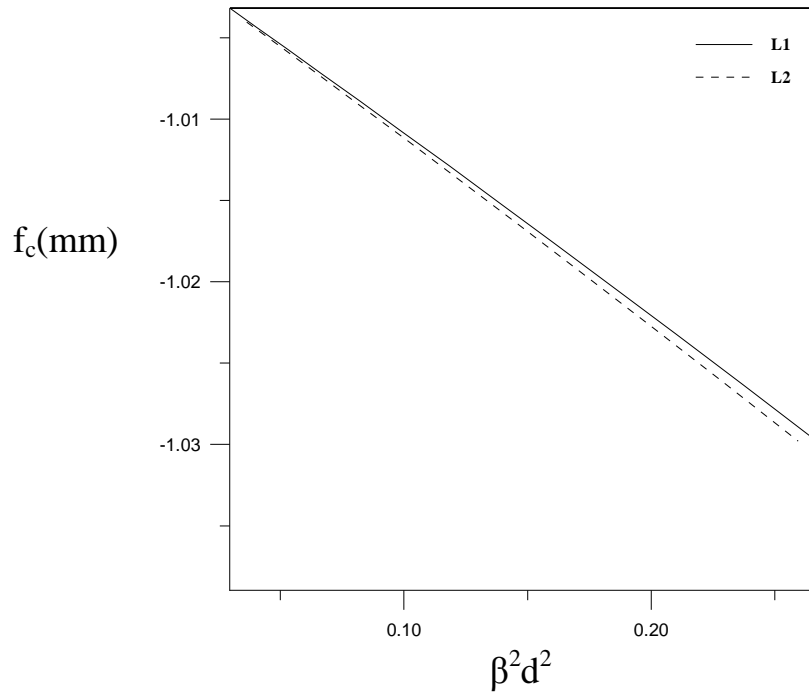


Figure (3-27): The focal length as a function of $\beta^2 d^2$ for the combined quadrupole lens in convergence plane for effective lengths of lens $L1=0.9\text{mm}$ and $L2=1\text{mm}$.

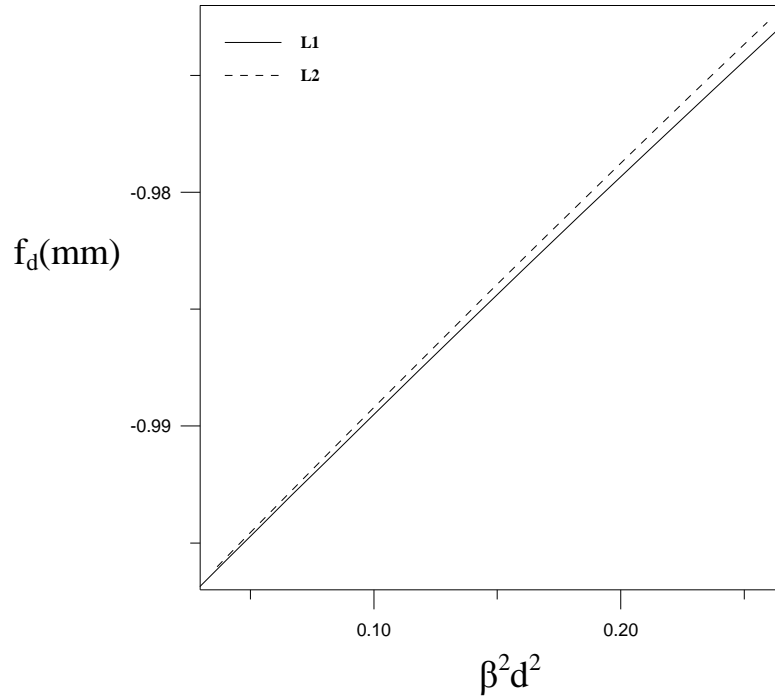


Figure (3-28): The focal length as a function of $\beta^2 d^2$ for the combined quadrupole lens in divergence plane for effective lengths of lens $L1=0.9\text{mm}$ and $L2=1\text{mm}$.

The relations between the focal length and the relative excitation parameter (n) for convergence and divergence planes, are shown in figures (3-29) and (3-30) respectively.

In figure (3-29) the focal length increases with relative excitation parameter (n) is increasing and the effective length of lens $L2 = 1\text{mm}$ has the values of focal length lower than that for $L1 = 0.9\text{mm}$. The inverse behaviour occurs for divergence plane as is shown in figure (3-30).

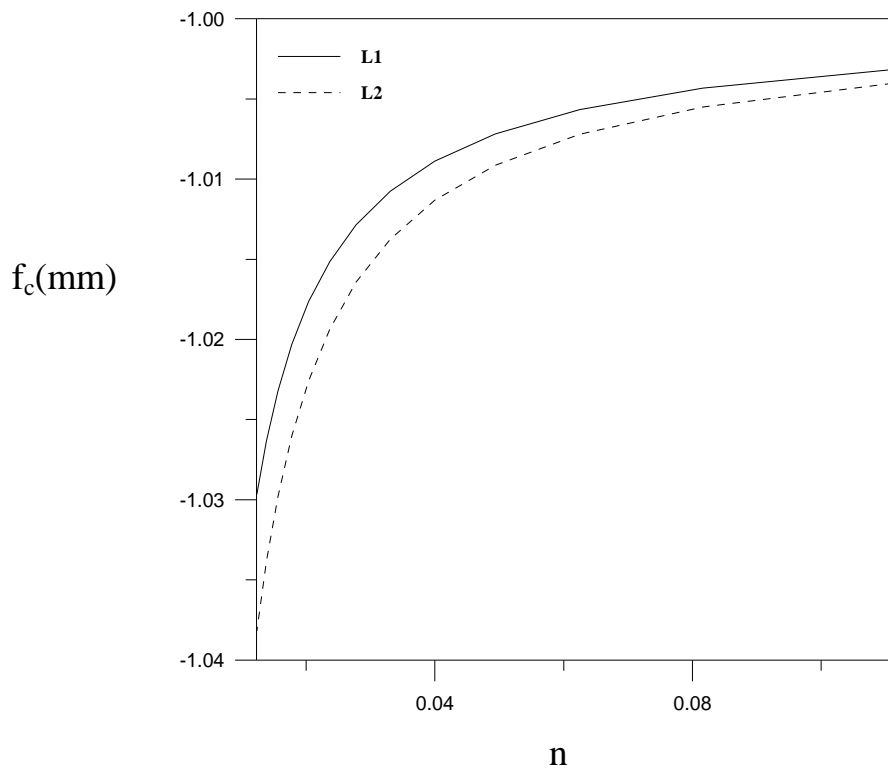


Figure (3-29): The focal length as a function of relative excitation parameter (n) for the combined quadrupole lens in convergence plane for effective lengths of lens $L1=0.9\text{mm}$ and $L2=1\text{mm}$.

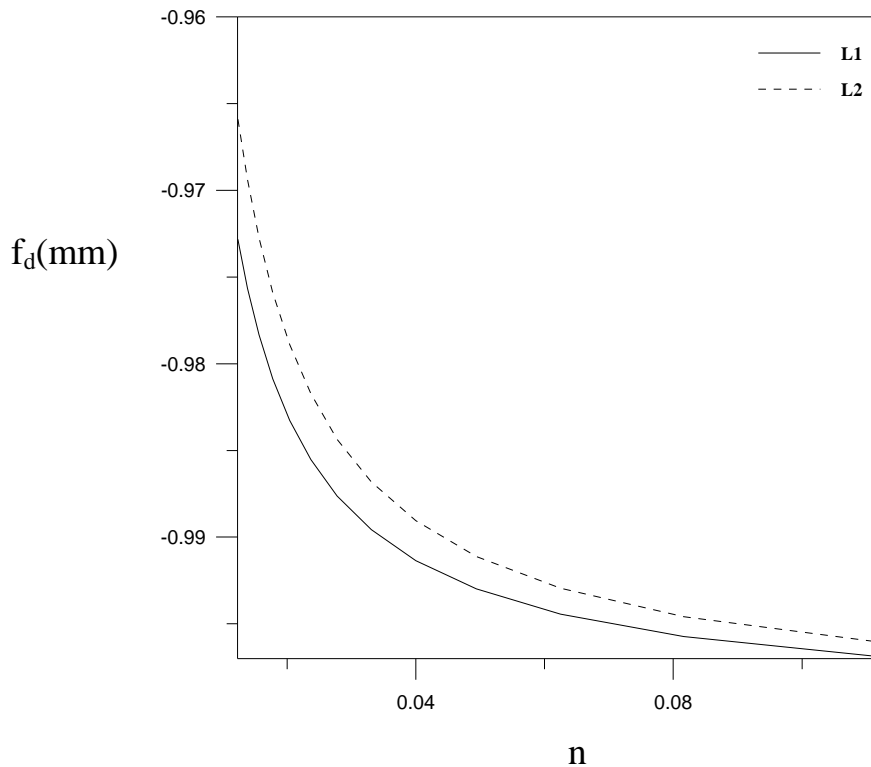
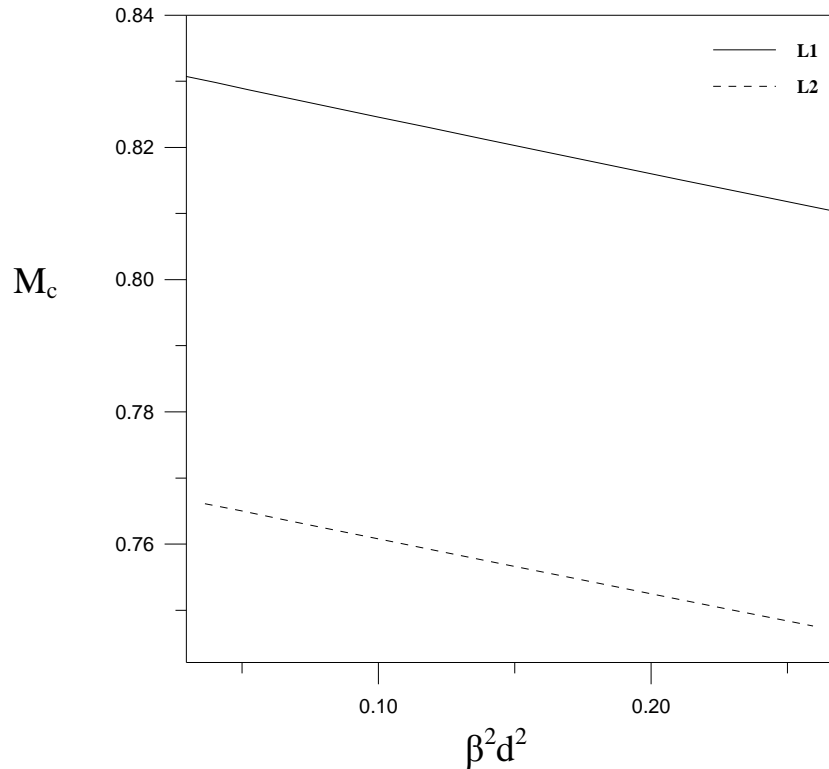


Figure (3-30): The focal length as a function of relative excitation parameter (n) for the combined quadrupole lens in divergence plane, for effective lengths of lens $L1=0.9\text{mm}$ and $L2=1\text{mm}$.

3-3-2-2 magnification

The effect of changing the effective length of lens on the magnification is investigated for both convergence and divergence planes, where the effective lengths $L1 = 0.9\text{mm}$ and $L2 = 1\text{mm}$ are taken into account and the relations between the magnification and $\beta^2 d^2$ are explained in figures (3-31) and (3-32), respectively.

From figure (3-31) the magnification decreases as $\beta^2 d^2$ is increasing and the values of magnification for effective length $L1(0.9\text{mm})$ greater than that of $L2(1\text{mm})$ and this behaviour is inversely to that of magnification in rectangular model.



Figure(3-31): The magnification as a function of $\beta^2 d^2$ for the combined quadrupole lens in convergence plane for effective lengths of lens $L1=0.9\text{mm}$ and $L2=1\text{mm}$.

In the case of divergence plane the results show opposite behaviour to the case of convergence plane, where the magnification increases with $\beta^2 d^2$ increases as is shown in figure (3-32). Also, the effective length $L1(0.9\text{mm})$ has the values of magnification greater than that of $L2(1\text{mm})$ and this behaviour is opposite to that for rectangular model.

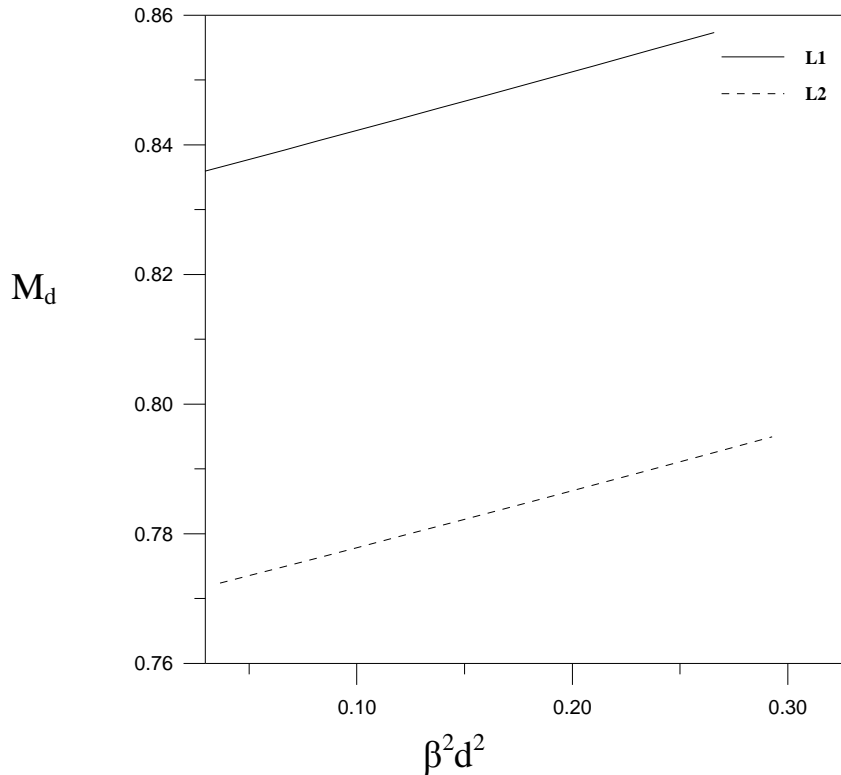
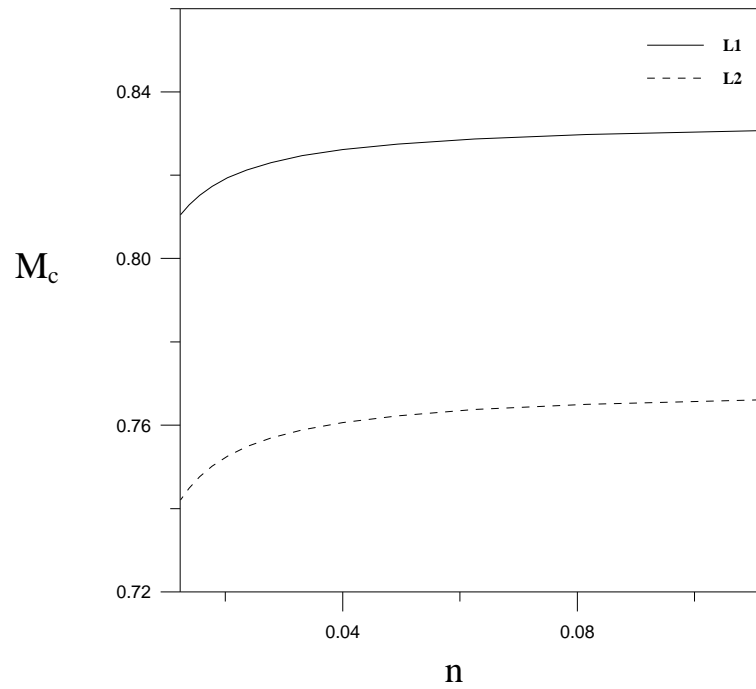


Figure (3-32): The magnification as a function of $\beta^2 d^2$ for the combined quadrupole lens in divergence plane for effective lengths of lens $L1=0.9\text{mm}$ and $L2=1\text{mm}$.

The relation between magnification and relative excitation parameter (n) is shown in figures (3-33) and (3-34) for both convergence and divergence planes, respectively. The figure (3-33) appears the increasing of magnification with increasing of relative excitation parameter (n) for convergence plane, while the opposite behaviour is found for magnification in divergence plane as is shown in figure (3-34).



Figure(3-33): The magnification as a function of relative excitation parameter (n) for the combined quadrupole lens in convergence plane for effective lengths of lens $L1=0.9\text{mm}$ and $L2=1\text{mm}$.

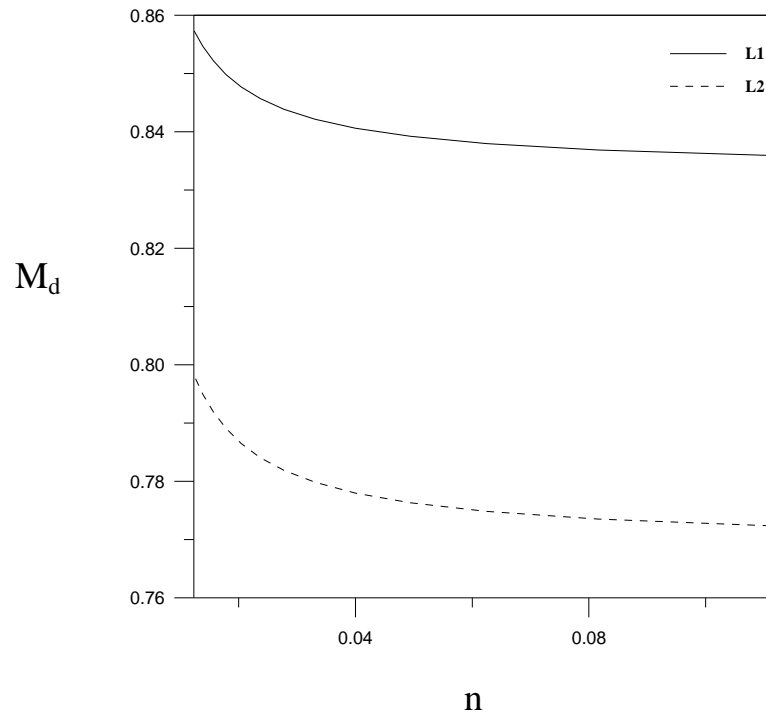


Figure (3-34): The magnification as a function of relative excitation parameter (n) for the combined quadrupole lens in divergence plane for effective lengths of lens $L1=0.9\text{mm}$ and $L2=1\text{mm}$.

3-3-3 The chromatic and spherical aberration for the combined quadrupole lens

3-3-3-1 the chromatic aberration

The optimization is made to find the optimum values of chromatic aberration coefficients in both convergence and divergence planes. The variation of effective length of lens are taken into account for two values, (L1(0.9mm) and L2(1mm)). The calculations in convergence plane are explained in figures (3-35) and (3-36). In figure (3-35) the relation between chromatic aberration coefficient C_{cx}/d and $\beta^2 d^2$ appears the increasing in chromatic aberration coefficient C_{cx}/d when $\beta^2 d^2$ increases up to $\beta^2 d^2 = 0.1$ for effective length of lens L1 = 0.9mm and $\beta^2 d^2 = 0.16$ for effective length of lens L2 = 1mm, and beyond these values the chromatic aberration coefficient C_{cx}/d decrease with increasing $\beta^2 d^2$

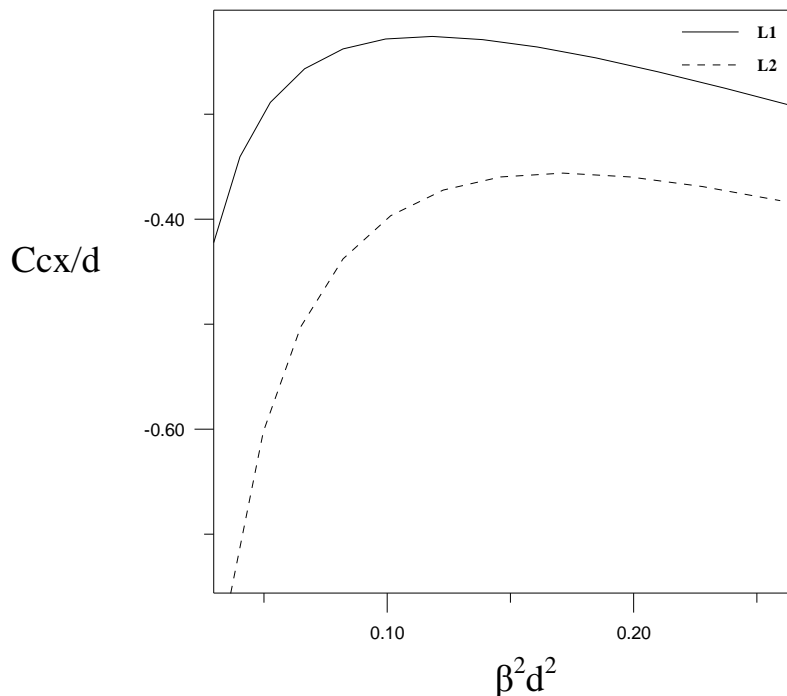


Figure (3-35): The relative chromatic aberration coefficients as a function of $\beta^2 d^2$ for the combined quadrupole lens in convergence plane for effective lengths of lens L1=0.9mm and L2=1mm.

The figure (3-36) appears the chromatic aberration coefficient change of magnification C_{mx} (for convergence plane) is decreasing with $\beta^2 d^2$ is increasing. The effective length of lens L2(1mm) has the values lower than that of L1(0.9mm).

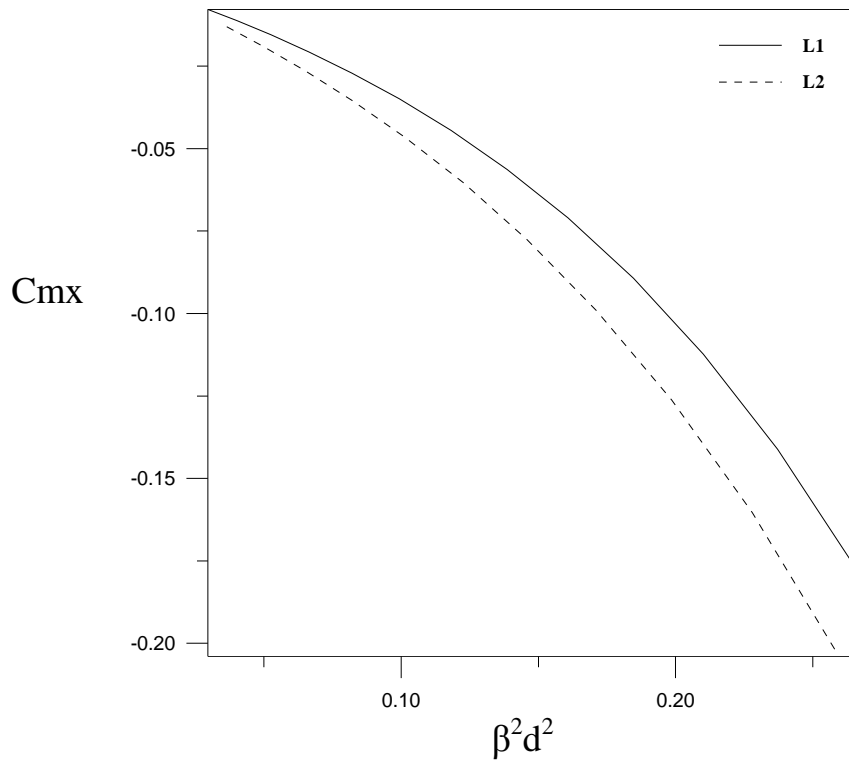


Figure (3-36): The relative chromatic aberration coefficients change of magnification as a function of $\beta^2 d^2$ for the combined quadrupole lens in convergence plane for effective lengths of lens L1=0.9mm and L2=1mm.

The results in divergence plane are shown in figures (3-37) and (3-38). The figure (3-37) shows the relation between chromatic aberration coefficient C_{cy}/d and $\beta^2 d^2$ and this relation has opposite behaviour to the calculations in convergence plane where C_{cx}/d decrease as $\beta^2 d^2$ increases up to $\beta^2 d^2 = 0.1$ for effective length of lens L1 and $\beta^2 d^2 = 0.145$ for effective length of lens L2, and beyond these values of $\beta^2 d^2$ the C_{cy}/d increases. . The effective length of lens

$L1 = 0.9\text{mm}$ has best values of C_{cy}/d for whole region of $\beta^2 d^2$ in compare with effective length of lens $L2 = 1\text{mm}$.

In figure (3-38) the chromatic aberration coefficient change of magnification C_{my} increases with $\beta^2 d^2$ is increasing and the effective length of lens $L1(0.9\text{mm})$ has the optimum results with respect to effective length of lens $L2(1\text{mm})$.

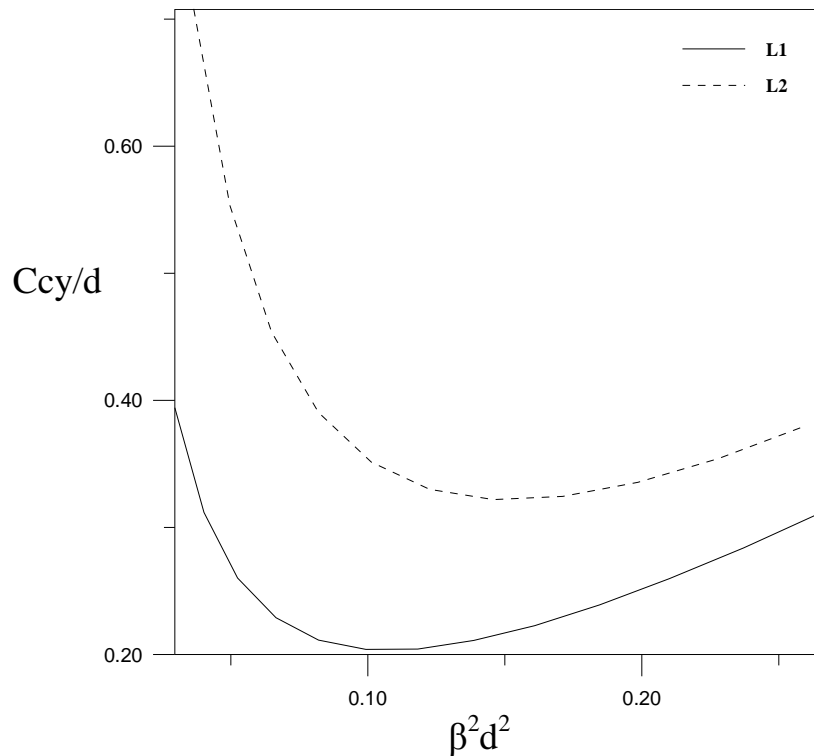


Figure (3-37): The relative chromatic aberration coefficients as a function of $\beta^2 d^2$ for the combined quadrupole lens in divergence plane for effective lengths of lens $L1=0.9\text{mm}$ and $L2=1\text{mm}$.

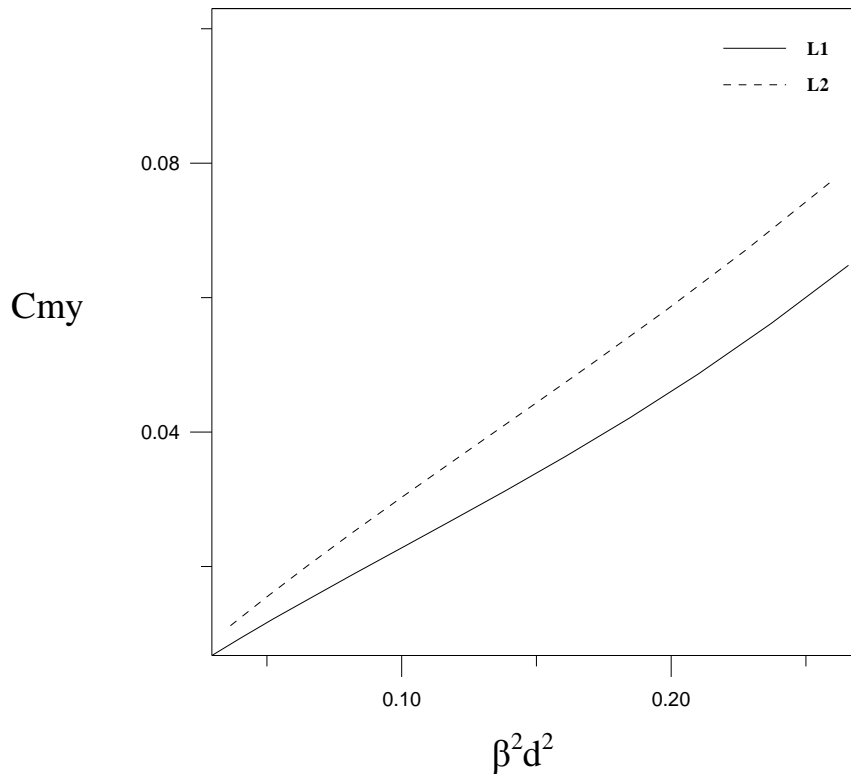


Figure (3-38): The relative chromatic aberration coefficients change of magnification as a function of $\beta^2 d^2$ for the combined quadrupole lens in divergence plane for effective lengths of lens $L1=0.9\text{mm}$ and $L2=1\text{mm}$.

The relation between chromatic aberration coefficients and relative excitation parameter (n) for both convergence and divergence planes, are studied. In figure (3-39) the chromatic aberration coefficient C_{cx}/d in convergence plane, increases as relative excitation parameter (n) increases at lower values of n and chromatic aberration coefficient C_{cx}/d decrease as relative excitation parameter increases beyond $n = 0.024$ for effective length of lens $L1(0.9\text{mm})$ and $n = 0.02$ for effective length of lens $L2(1\text{mm})$ and the effective length of lens $L2 = 1\text{mm}$ gives the best values of C_{cx}/d . Also the C_{cx}/d has the negative values for whole rang of relative excitation parameter (n). The opposite behaviour is found for the case of divergence plane as is shown in figure (3-41).

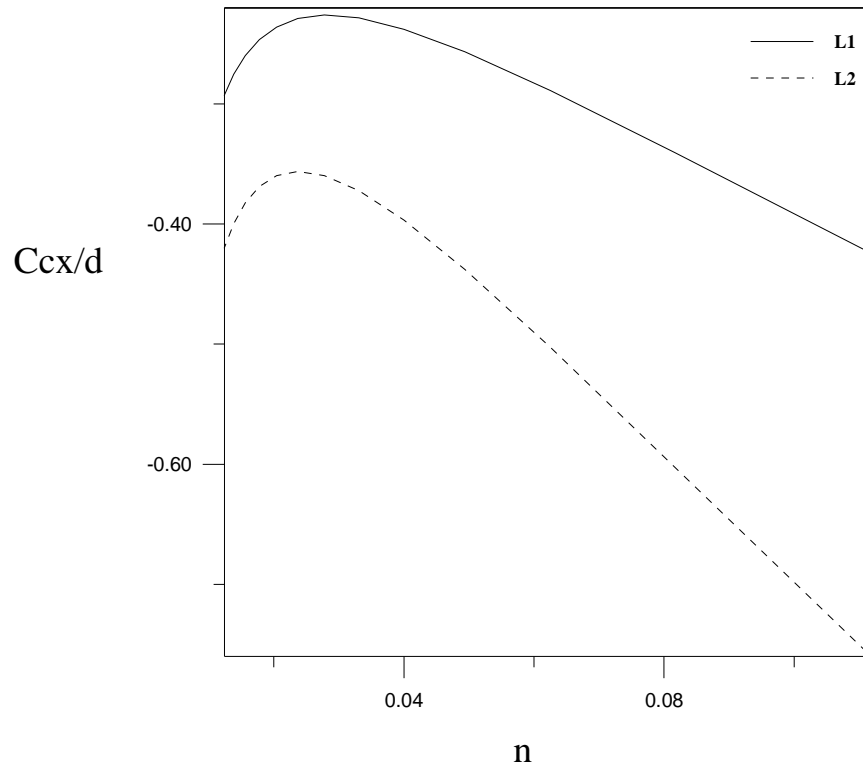


Figure (3-39): The relative chromatic aberration coefficients as a function of relative excitation parameter (n) for the combined quadrupole lens in convergence plane for effective lengths of lens $L1=0.9\text{mm}$ and $L2=1\text{mm}$.

The results in figure (3-40) show the relation between chromatic aberration coefficient change of magnification C_{mx} and relative excitation parameter (n) for effective lengths of lens. From the figure, the chromatic aberration coefficient change of magnification C_{mx} increases with increasing relative excitation parameter (n) and for effective length of lens $L2$ give us the optimum result in compare with $L1$.

The opposite behaviour for chromatic aberration coefficient change of magnification is found for the case of divergence plane and the result is explained in figure (3-42).

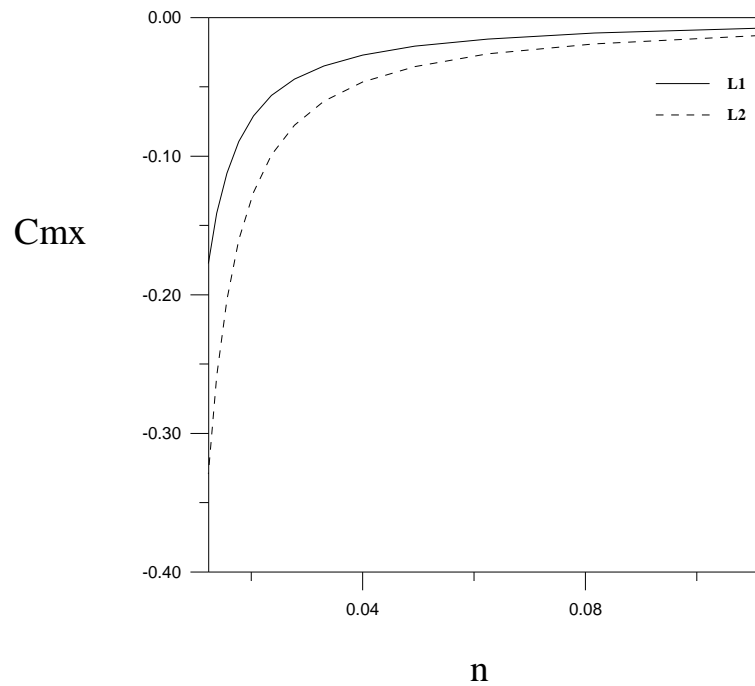


Figure (3-40): The relative chromatic aberration coefficients change of magnification as a function of relative excitation parameter (n) for the combined quadrupole lens in convergence plane for effective lengths of lens $L1=0.9\text{mm}$ and $L2=1\text{mm}$.

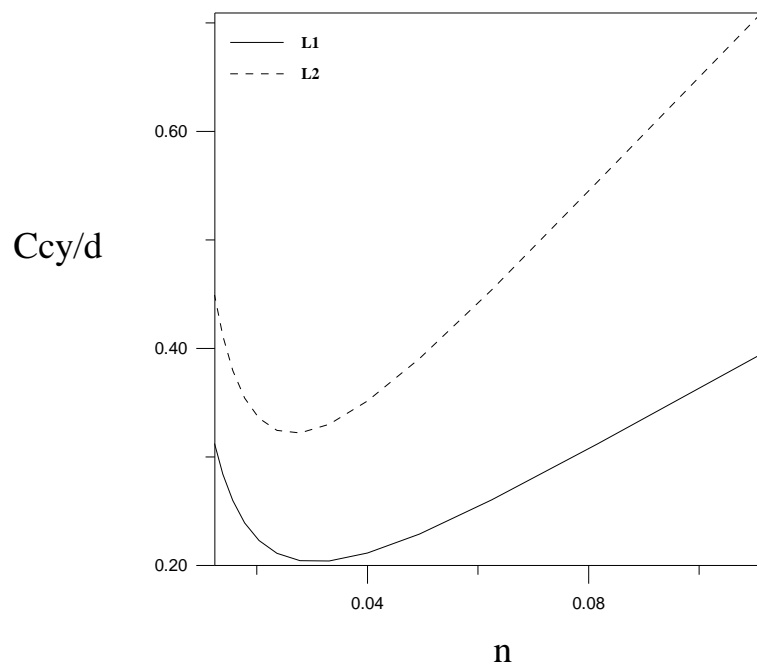


Figure (3-41): The relative chromatic aberration coefficients as a function of relative excitation parameter (n) for the combined quadrupole lens in divergence plane for effective lengths of lens $L1=0.9\text{mm}$ and $L2=1\text{mm}$.

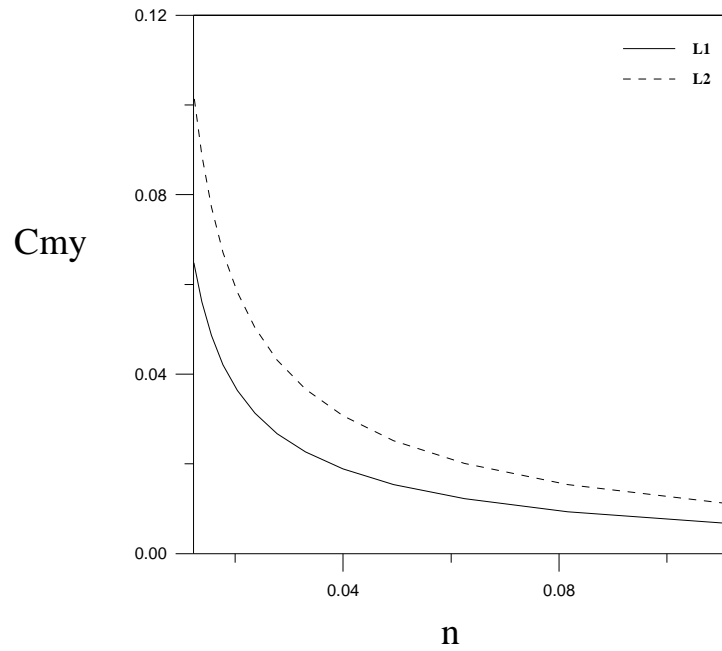


Figure (3-42): The relative chromatic aberration coefficients change of magnification as a function of relative excitation parameter (n) for the combined quadrupole lens in divergence plane for effective lengths of lens $L1=0.9\text{mm}$ and $L2=1\text{mm}$.

3-3-3-2 the spherical aberration

After finding the optimum result for the case of achromatic aberration under this model of field distribution the present aim in this section is finding the optimum values of spherical aberration coefficients in both convergence and divergence plane and study the effects of changing the excitation parameter and effective length of lens on this coefficient. For the convergence plane the results are shown in figures (3-43) and (3-44). The calculations in the figure (3-43) appear the relation between spherical aberration coefficient C_{30}/d as the function of $\beta^2 d^2$ and this coefficient is decreasing with increasing $\beta^2 d^2$. All the values of spherical aberration coefficient C_{30}/d have the negative values and the effective length $L1(0.9\text{mm})$ has values lower than that of $L2(1\text{mm})$. The figure (3-44) explains the spherical aberration coefficient C_{12}/d this coefficient increases with $\beta^2 d^2$ is increasing. The effective length $L1(0.9\text{mm})$ has values greater than that of $L2(1\text{mm})$.

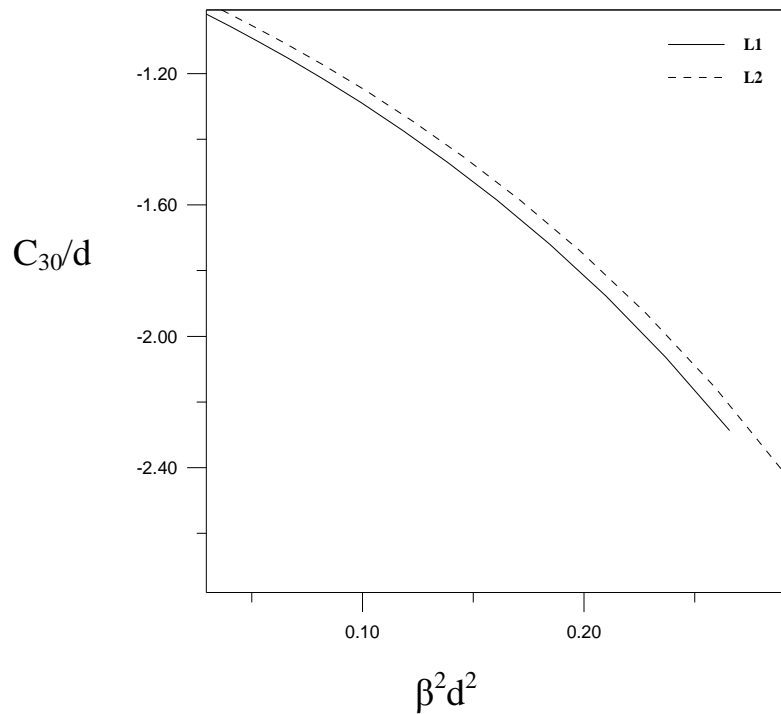


Figure (3-43): The relative spherical aberration coefficients C_{30}/d as a function of $\beta^2 d^2$ for the combined quadrupole lens in convergence plane for effective lengths of lens $L1=0.9\text{mm}$ and $L2=1\text{mm}$.

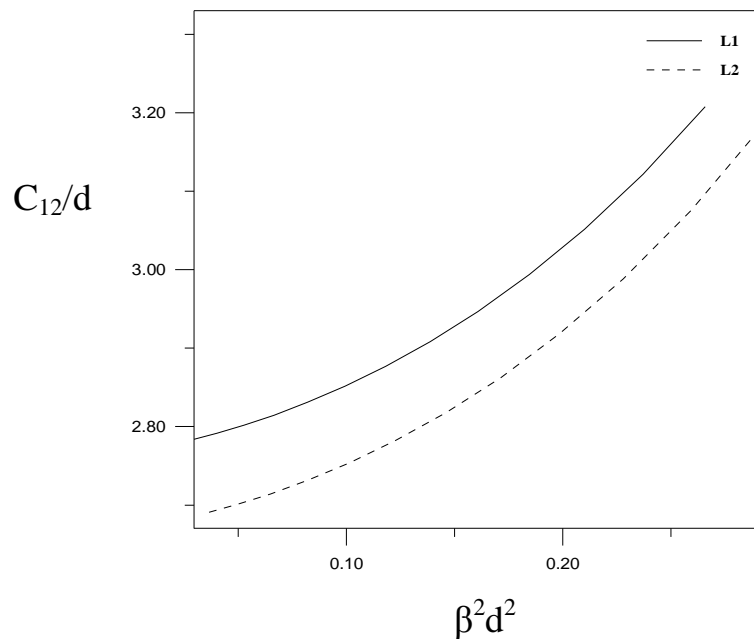


Figure (3-44): The relative spherical aberration coefficients C_{12}/d as a function of $\beta^2 d^2$ for the combined quadrupole lens in convergence plane for effective lengths of lens $L1=0.9\text{mm}$ and $L2=1\text{mm}$.

In the case of divergence plane in the results are shown in figures (3-45) and (3-46). The calculations of figure (3-45) show that the spherical aberration coefficient D_{03}/d increases with increasing $\beta^2 d^2$ and the all values of this coefficient are negative for whole range of $\beta^2 d^2$. Also, the effective length L1(0.9mm) gives best results in compare with L2(1mm). The results of spherical aberration coefficient D_{21}/d have the same description to that of spherical aberration coefficient D_{03}/d but the difference that, all the values of spherical aberration coefficient D_{21}/d are positive as is shown in figure (3-46).

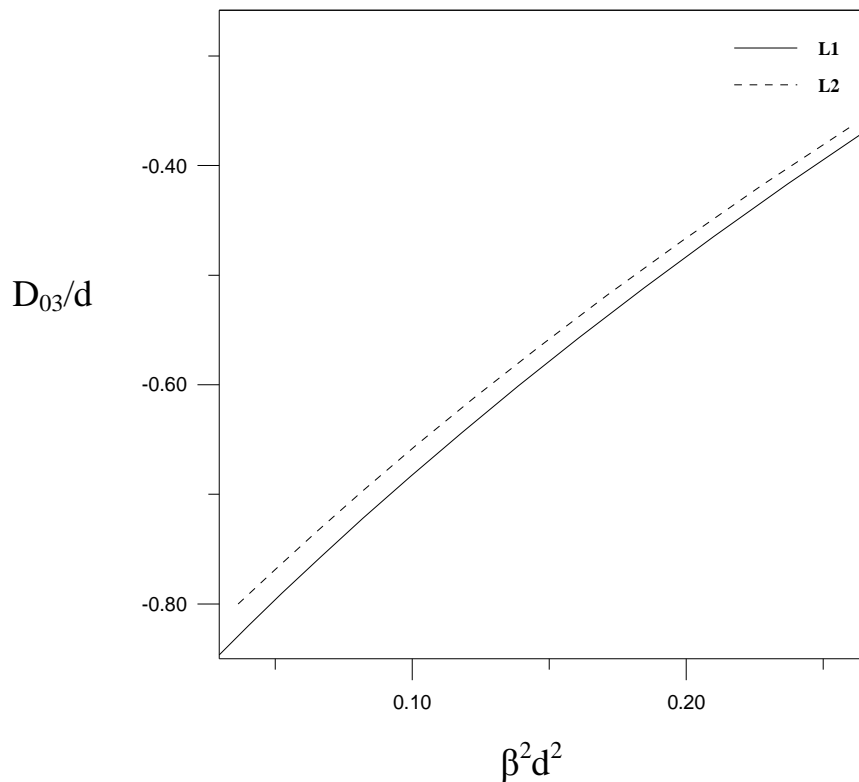


Figure (3-45): The relative spherical aberration coefficients D_{03}/d as a function of $\beta^2 d^2$ for the combined quadrupole lens in divergence plane for effective lengths of lens L1=0.9mm and L2=1mm.

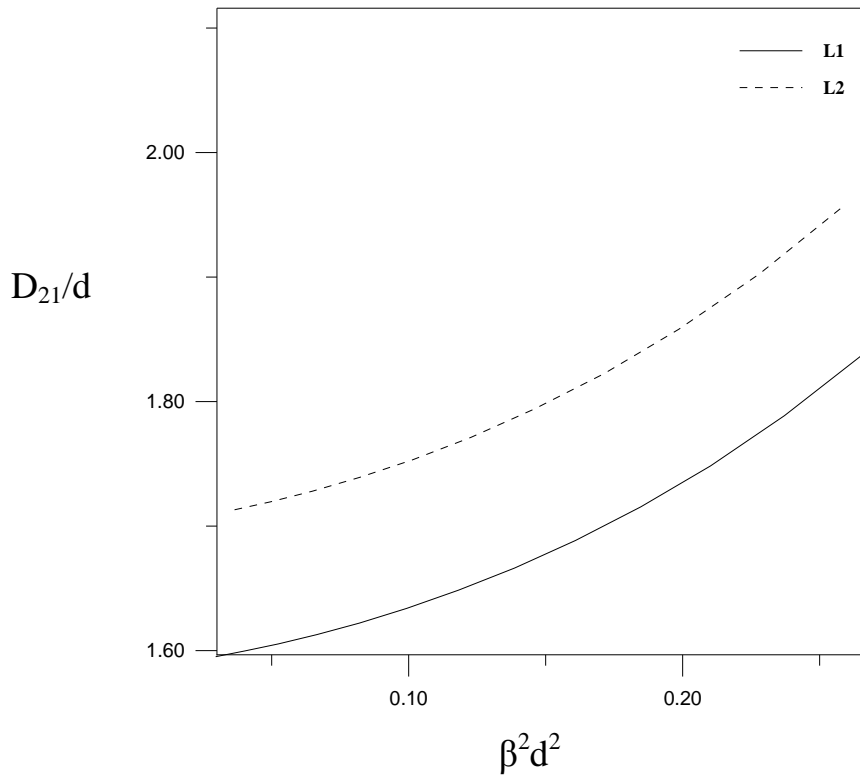


Figure (3-46): The relative spherical aberration coefficients D_{21}/d as a function of $\beta^2 d^2$ for the combined quadrupole lens in divergence plane for effective lengths of lens $L1=0.9\text{mm}$ and $L2=1\text{mm}$.

The relation of spherical aberration coefficients with relative excitation parameter (n) in both convergence and divergence planes is shown in figures (3-47) to (3-50). The figures (3-47) and (3-48) show this relation in convergence plane. The values of spherical aberration coefficient C_{30}/d become greater with n is increasing as is shown in figure (3-47). While the opposite behaviour is found for spherical aberration coefficient C_{12}/d as is shown in figure (3-48).

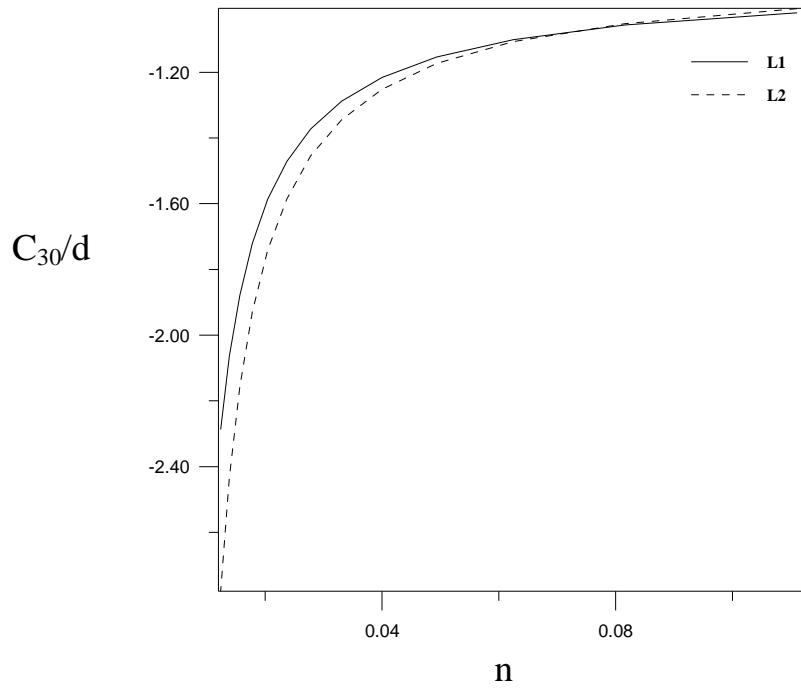
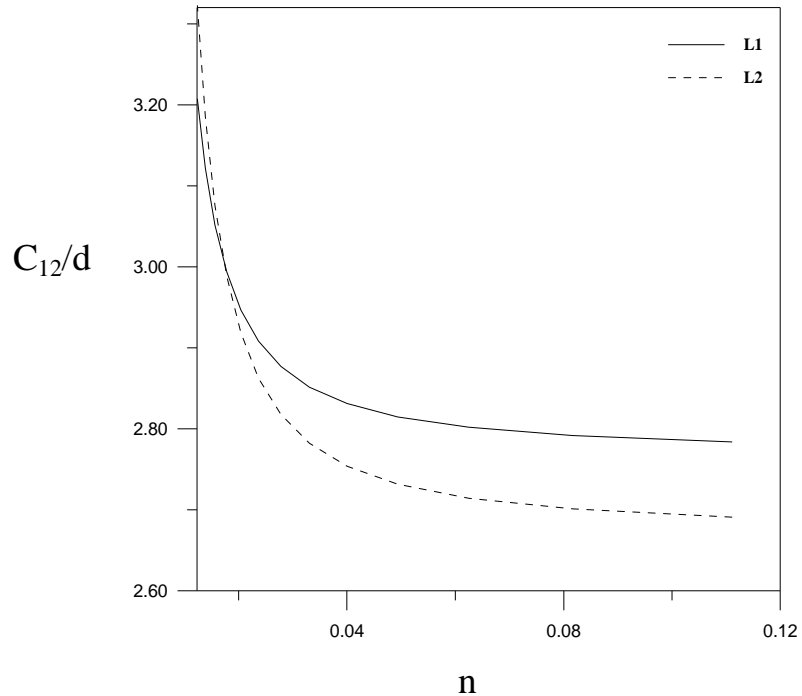


Figure (3-47): The relative spherical aberration coefficients C_{30}/d as a function of relative excitation parameter (n) for the combined quadrupole lens in convergence plane for effective lengths of lens $L1=0.9\text{mm}$ and $L2=1\text{mm}$.



Figure(3-48): The relative spherical aberration coefficients C_{12}/d as a function of relative excitation parameter (n) for the combined quadrupole lens in convergence plane for effective lengths of lens $L1=0.9\text{mm}$ and $L2=1\text{mm}$.

In the case divergence plane, the results are explained in figures (3-49) and (3-50). For both spherical aberration coefficients D_{03}/d and D_{21}/d the inverse relation between these coefficient and the relative excitation parameter (n) is found as is shown in figures.

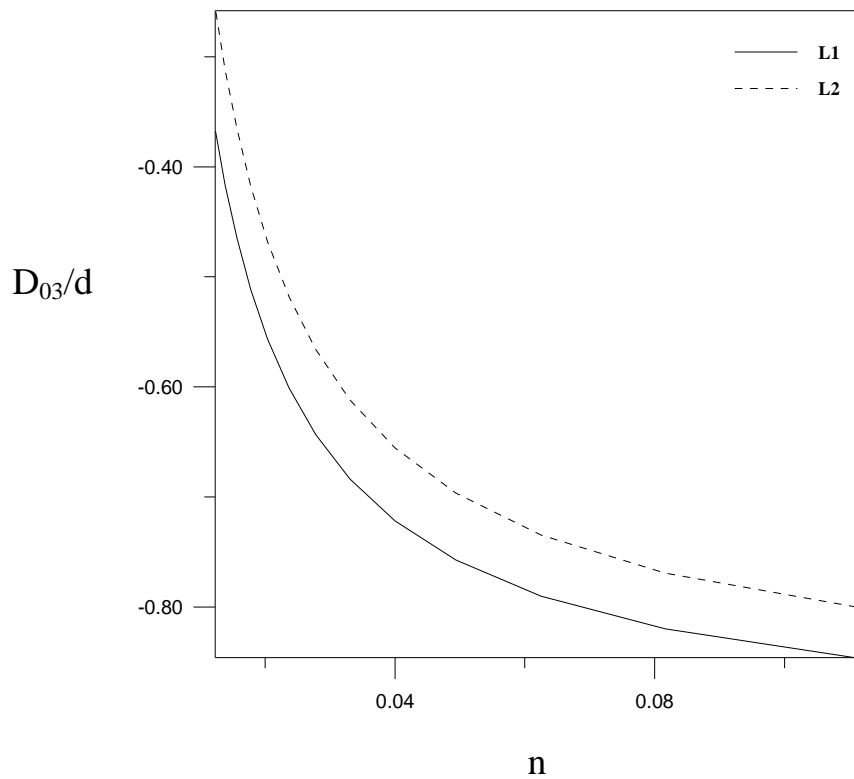


Figure (3-49): The relative spherical aberration coefficients D_{03}/d as a function of relative excitation parameter (n) for the combined quadrupole lens in divergence plane for effective lengths of lens $L1=0.9\text{mm}$ and $L2=1\text{mm}$.

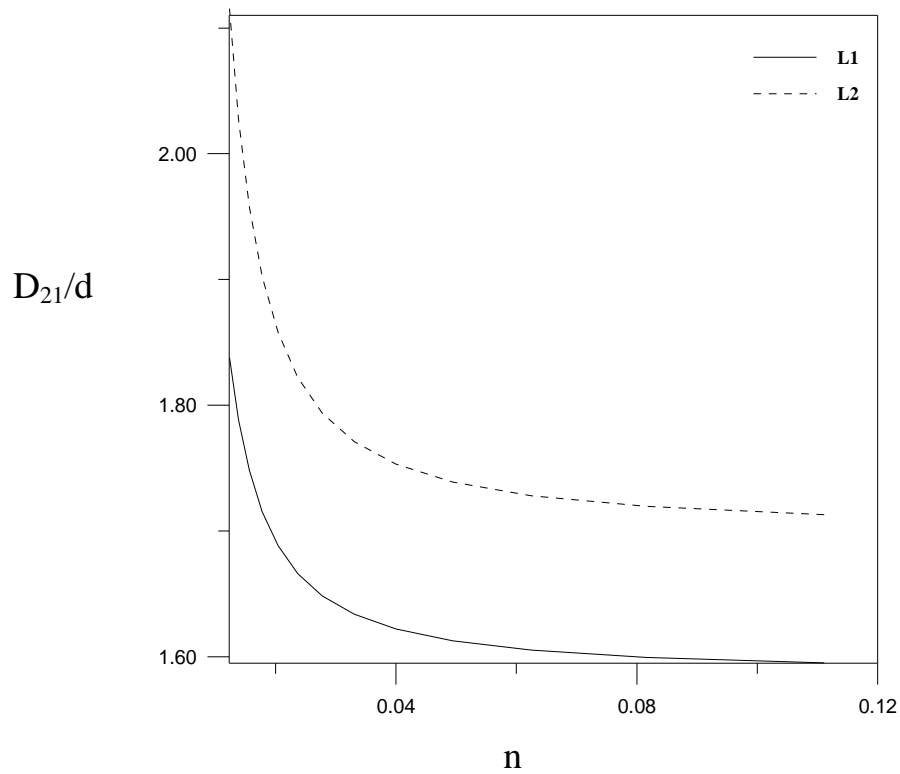


Figure (3-50): The relative spherical aberration coefficients D_{21}/d as a function of relative excitation parameter (n) for the combine quadrupole lens in divergence plane for effective lengths of lens $L1=0.9\text{mm}$ and $L2=1\text{mm}$.

4.1 Conclusions

Combined quadrupole lens is proposed and investigated which is formed by an electrostatic and magnetic fields imposed on each other. It appears that the rectangular model and bell-shaped model can be used to represent the axial field distribution of the combined quadrupole lens to find the optimum design of the achromatic lens. The combined quadrupole lens has many variable geometrical and operational parameters. However, from the present investigation one can conclude the following:

1. The calculations of rectangular model and bell-shaped model in both convergence and divergence show that the values of the focal length and magnification are closer to each other for both values of the effective lengths of lens ($L_1 = 0.9\text{mm}$ and $L_2 = 1\text{mm}$).
2. The chromatic aberration coefficients of the rectangular and bell-shaped models for the effective length of lens $L_1(0.9\text{mm})$ is lower than that of the effective length of lens $L_2(1\text{mm})$. In the case of spherical aberration opposite behaviour is found.
3. The rectangular model is a good model to give the achromatic aberration in combined quadrupole lens.
4. From the calculations it is found that the chromatic aberration coefficients can be reduced to zero value but the problems are values of the focal lengths are very large and at the same time the effective length and excitation of lens is very small and that does not satisfy the optimum design.

4.2 Recommendations for Future Work

The following topics can be recommended for future work:

- (a) Studing the effect of the relativistic velocities of the charged particles on the design and properties of combined quadrupole lens.
- (b) Studing the effect of charged-particles initial energy on the optical properties of the combined electrostatic and magnetic quadrupole lens.
- (c) Studing the design of achromatic lens on doublet, triplet and quadruplet consisting of an electrostatic and magnetic quadrupole lens.
- (d) Studing the effect of other types of the electrode on the properties of electrostatic and magnetic quadrupole lens.
- (e) Studing the effect of other types of the axial field distribution model on the the properties of combined quadrupole lens.
- (f) Studing the design of achromatic lens of combined octupole and quadrupole lens.

Contents

Abstract iv

List of Symbols vi

1- INRODUCTION

1-1 Electrostatic and Magnetic Quadrupole Lenses 1

1-2 Achromatic Quadrupole Lens 3

1-3 Historical Development 6

1-4 Aim of the Project 9

2- THEORETICAL CONSIDERATIONS

2-1 Field Models For Quadrupole Lenses 10

2-2 The Paraxial Ray Equation of Motion and The First–Order
Optical Properties 13

2-2-1 The rectangular model 13

2-2-2 The bell-shaped 19

2-3 Lens Aberration Parameters 24

2-3-1 Chromatic aberration 26

2-3-1-1 rectangular model 27

2-3-1-2 bell-shaped model 28

2-3-2 Spherical aberration 29

2-3-2-1 rectangular model 30

2-3-2-2 bell-shaped model 31

2-4 Computer Program for Computing The Beam Trajectory,	33
The Optical Properties and Aberration Coefficients of Combined Quadrupole Lens	

3- RESULTS AND DISCUSSION

3-1 Introduction	35
3-2 Rectangular Model	35
3-2-1 Trajectory equation of motion of charged particles for the combined quadrupole lens	35
3-2-2 Optical properties for the combined quadrupole lens	37
3-2-2-1 focal length	37
3-2-2-2 magnification	41
3-2-3 The chromatic and spherical aberration for the combined quadrupole lens	45
3-2-3-1 the chromatic aberration	45
3-2-3-2 the spherical aberration	53
3-3 Bell-Shaped Model	60
3-3-1 Trajectory equation of motion of charge particles for the combined quadrupole lens	60
3-3-2 Optical properties for the combined quadrupole lens	61
3-3-2-1 focal length	61
3-3-2-2 magnification	64

3-3-3 The chromatic and spherical aberration for the combined quadrupole lens	68
3-3-3-1 the chromatic aberration	68
3-3-3-2 the spherical aberration	74

4- CONCLUSIONS AND RECOMMENDATIONS FOR FUTURE WORK

4-1 Conclusions	81
4-2 Recommendations for Future Work	82
References	83

Examination Committee Certification

We certify that we have read the thesis entitled **Investigation of The Optical Properties of The Achromatic Quadrupole Lens**, and as an examination committee, examined the student **Fatma Nafaa Gaafer Al-Zubaidy** on its contents, and that in our opinion it is adequate for the partial fulfillment of the requirements for the degree of **Master of Science in Physics**.

Signature:

Name: Dr. Ahmad K. Ahmad (Chairman)

Title: Assistant professor

Date: / / 2007

Signature:

Name: Dr. Mohammed I. Sanduk (Member)

Title: Assistant professor

Date: / / 2007

Signature:

Name: Dr. Samir K. Al-Ani (Member)

Title: Assistant professor

Date: / / 2007

Signature:

Name: Dr. Fatin A. J. Al-Moudarris
(Supervisor)

Title: Lecturer

Date: / / 2007

Signature:

Name: Dr. Uday A. H. Al-Obaidy
(Supervisor)

Title: Lecturer

Date: / / 2007

Approved by the University Committee of Postgraduate Studies

Signature:

Name: Dr. Laith Abdul Aziz Al-Ani

Title : Assistant professor

Dean of College of Science

Date: / / 2007

List of Symbols

c Aperture radius of the quadrupole lens (bore-radius) (mm).

C_{cx}, C_{cy}	Chromatic aberration coefficients of combined quadrupole lens in convergence and divergence planes, respectively (mm).
C_{mx}, C_{my}	Chromatic aberration coefficients change of magnification of combined quadrupole lens in convergence and divergence planes, respectively.
C_{30}, C_{12}	Spherical aberration coefficients of combined quadrupole lens in the convergence plane.
d	The axial extension of the field (mm).
D_{03}, D_{21}	Spherical aberration coefficients of combined quadrupole lens in the divergence plane.
$f(z)$	The function of the field distribution.
f_c, f_d	Focal lengths in the convergence and divergence planes, respectively (mm).
f_i, f_o	Focal lengths in the image and object side, respectively (mm).
H_{ic}, H_{id}	Principal planes in image side of convergence and divergence planes, respectively.
H_{oc}, H_{od}	Principal planes in object side of convergence and divergence planes, respectively.
k	A coefficient accounting for the shaped of the electrode.
L	Effective length(mm).
ℓ	Electrode length (mm).
M_c, M_d	Magnification of quadrupole lens in the convergence and divergence planes, respectively.
m_c, m_d	Reciprocal magnification of quadrupole lens in the convergence and divergence planes, respectively.
T_c, T_d	Transfer matrices of the quadrupole lens in the convergence and divergence planes, respectively.
u	Object distance (mm).

v	Image distance (mm).
$\Delta V, V$	The potential distribution (volt).
z	Optical axis (mm).
Z_{ic}, Z_{id}	Focal planes in image side of convergence and divergence planes, respectively.
Z_{oc}, Z_{od}	Focal planes in object side of convergence and divergence planes, respectively.
β	Lens excitation (mm^{-1}).
β_e, β_m	The excitation of electric and magnetic lenses respectively (mm^{-1}).
α, γ	The image side semi-aperture angles in the x-z and y-z planes, respectively.

References

- Baranova, L.A. and Yavor, S.Ya. (1984)
Electrostatic lenses
Sov. Phys. – Tech. Phys., **29**(8), 827-845

- Baranova, L.A. and Read, F.H. (1998)
Reduction of the chromatic and aperture aberrations of the stigmatic quadrupole lens triplet
Optik, **109**(1), 15-21

- Baranova, L.A. and Read, F.H. (1999)
Minimisation of the aberrations of electrostatic lens systems composed of quadrupole and octupole lenses
International Journal of Mass Spectrometry, **189**, 19-26

- Baranova, L.A. and Read, F.H. (2001)
Aberrations caused by mechanical misalignments in electrostatic quadrupole lens systems
Optik, **112**(3), 131-138

- Dymnikov, A.D., Ovsyannikova, L.P. and Yavor, S.Ya. (1963)
Systems of quadrupole lenses
Sov. Phys. – Tech. Phys., **8**(4), 293-296

- Dymnikov, A.D., Fishkova, T.Ya and Yavor, S.Ya. (1965)
Spherical aberration of compound quadrupole lenses and systems
Nucl. Instrum. Meth., **37**, 268-275

- Dymnikov, A.D., Fishkova, T.Ya and Yavor, S.Ya. (1965)
Spherical aberration of a quadrupole lens combined with a rectangular field distribution
Sov. Phys. – Dok., **10**(6), 547-550

- Dymnikov, A.D., Glass, G.A. and Rout, B. (2005)
Zoom quadrupole focusing systems producing an image of an object
Nuclear Instruments and Methods in Physics Research, **B241**, 402- 408

- Fishkova, T.Ya., Baranova, L.A. and Yavor, S.Ya. (1968)
Spherical aberration of a stigmatic doublet of quadrupole lenses (rectangular model)
Sov. Phys. – Tech. Phys., **13**, 520-525

- Grivet, P. (1972)
Electron optics
(Pergamon Press, Oxford and New York)

- Grime, G.W. and Watt, F. (1988)
Focusing protons and light ions to micron and submicron dimensions
Nuclear Instruments and Methods in Physics Research, **B30**, 227-234

- Hawkes, P.W. (1965)
The paraxial chromatic aberrations of rectilinear orthogonal systems
Optik, **22**, 543-554

- Hawkes, P.W. (1965/1966)
The electron optics of a quadrupole lens with triangular potential
Optik, **23**, 145-168

- Hawkes, P.W. (1967)
Asymptotic quadrupole aberrations: the bell-shaped model (I)
Optik, **25**, 439-458

- Hawkes, P.W. (1967/1968)
Asymptotic quadrupole aberrations: the bell-shaped model (III)
Optik, **26**, 507-552

- Hawkes, P.W. (1970)
Quadrupole in electron lens design
Advances in Electronics and Electron Physics, Supplement 7, ed. Marton, L.
(Academic Press, New York and London).

- Harriott, L.R., Brown, W.L. and Barr, D.L. (1990)
Anticipated performance of achromatic quadrupole focusing systems when used with liquid metal ion sources
Journal of Vacuum Science and Technology A: Vacuum, Surfaces, and Films, **8**(4), 3279-3283

- Jamieson, D.N. and Legge, G.J.F. (1987)
Aberrations of single magnetic quadrupole lenses
Nuclear Instruments and Methods in Physics Research, **B29**, 544-556

- Jamieson, D.N. and Tapper, U.A.S. (1989)
Grid shadow pattern analysis of achromatic quadrupole lenses
Nuclear Instruments and Methods in Physics Research, **B44**, 227-232

- Larson, J.D. (1981)
Electrostatic ion optics and beam transport for ion implantation
Nucl. Instrum. Meth., **189**, 71-91

- Moses, R.W., JR. (1970)
Minimum aperture aberrations of quadrupole lens systems
The Review of Scientific Instruments, **41**(5), 729-740

- Moses, R.W., JR. (1971)
Minimum chromatic aberrations of magnetic quadrupole objective lenses
The Review of Scientific Instruments, **42**(6), 828-831

- Markovich, M.G. (1972)
Short quadrupole, hexapole, and octupole lenses as aberration correctors for electron- beam deflection
Sov. Phys. – Tech. Phys., **17**(1), 30-33

- Martin, F.W. and Goloskie, R. (1982)
An achromatic quadrupole lens doublet for positive ions
Appl. Phys. Lett., **40**(2), 191-193

- Martin, F.W. and Goloskie, R. (1982)
Achromatic proton microbeams
Nucl. Instrum. Meth., **197**, 111-116

- Ovsyannikova, L.P. (1968)
Dependence of geometric aberration of slant beams in a quadrupole lens on the degree of its excitation
Radio Engineering and Electronic Physics, **13**(8), 1292-1294

- Okayama, S. (1989)
Electron beam lithography using a new quadrupole triplet
SPIE, Electron-beam, X-ray, and Ion-beam Technology: Submicrometer Lithographies VIII, **1089**, PP 74-83

- Okayama, S. (1990)
A new type of quadrupole correction lens for electron-beam lithography
Nuclear Instruments and Methods in Physics Research, **A298**, 488-495

- Ovsyannikova, L.P. and Fishkova, T.Ya. (2001)
A simple quadrupole-octupole electromagnetic lens
Technical Physics, **46**(5), 601-604

- Rose, H. (2003)
Outline of an ultracorrector compensating for all primary chromatic and geometrical aberrations of charged – particle lenses
Microsc. Microanal., **9**, 32

- Rose, H. and Wan, W. (2005)
Aberration correction in electron microscopy
IEEE, Proceedings of 2005 Particle Accelerator Conference, Knoxville, Tennessee.

- Shpak, E.V. and Yavor, S.Ya. (1965)
Achromatic electromagnetic quadrupole lens with noncoincident axial field distribution
Sov. Phys. – Tech. Phys., **10**, 727-729

- Szilagyi, M., Blaschta, F, Ovsyannikova, L.P. and Yavor, S.Ya. (1973)
Analytical expressions for all third-order aberration coefficients of quadrupole lenses. Bell-shaped model
Optik, **38**(4), 416-424

- Szabo, Gy. (1975)
Geometrical aberration of the combination of asymmetrically fed quadrupole lenses and magnetic sectors
Nucl. Instrum. Meth., **125**, 339-343

- Szilagyi, M. (1988)
Electron and ion optics
(Plenum Press, New York)

- Shimizu, H., Currell, F.J., Ohtani, S., Sokell, E.J., Yamada, C., Hirayama, T. and Sakurai, M. (2000)
Characteristics of the beam line at the Tokyo electron beam ion trap
The Review of Scientific Instruments, **71**(2), 681-683

- Tapper, U.A.S. (1991)
Achromatic focusing for probeforming of high resolution microbeam
Nuclear Instruments and Methods in Physics Research, **B56-57**, 712-716

- Yavor, S.Ya., Dymnikov, A.D. and Ovsyannikova, L.P. (1964)
Achromatic quadrupole lenses
Nucl. Instrum. Meth., **26**, 13-17

- Yavor, S.Ya. and Dymnikov, A.D. (1964)
Achromatic multipole lenses
Sov. Phys. – Dok., **9**(2), 177-178

- Yavor, S.Ya., Ovsyannikova, L.P. and Baranova, L.A. (1972)
Correction of geometrical aberrations in electron-optical systems by octupoles
Nucl. Instrum. Meth., **99**, 103-108

الخلاصة

حسابات الامثلية أجريت لايجاد افضل خواص لعدسة رباعية مركبة مكونة من عدسة كهروسكونية ومغناطيسية. الخواص البصرية حسبت حيث حسب كل من البعد البؤري والتكبير. كلا الزيغين اللوني والكروي أختزلا لاقل قيم والزيغ اللالوني وجد لحالات عدة.

الحسابات أنجزت بالاستعانة بطريقة المصفوفات الانتقالية وباستخدام كل من الانموذجين المستطيلي والناقوسي الشكل لتوزيع المجال، حيث حسب مسار الجسيمات المشحونة التي تعبر المجال بحل معادلة مسار الحركة ثم حسبت الخواص البصرية للعدسة بمساعدة مسار الحزمة على امتداد محور العدسة.

الحسابات ركزت على ايجاد البعد البؤري والتكبير والزيغين اللوني والكروي لكلا المستويين التقاربي والتباعدي، وكذلك تأثيرات تغير التهيج للعدسة وطولها الفعال درست وأخذت بنظر الاعتبار.



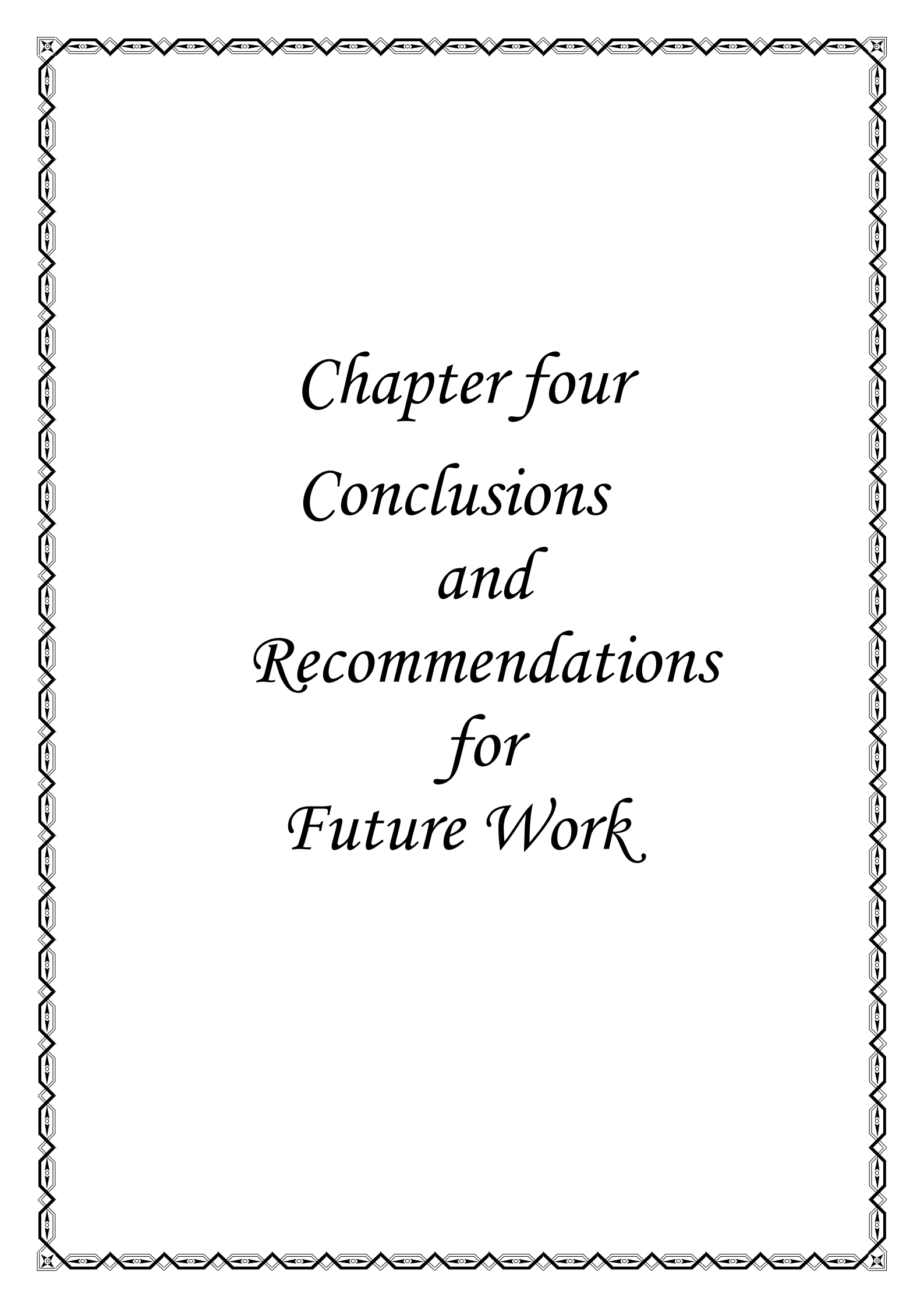
Chapter One
Introduction



Chapter Two
Theoretical considerations



Chapter Three
Results and Discussion



Chapter four
Conclusions
and
Recommendations
for
Future Work



References

Republic of Iraq
Ministry of Higher Education and Scientific Research
Al-Nahrain University
College of Science
Department of Physics



INVESTIGATION OF THE OPTICAL PROPERTIES OF THE ACHROMATIC QUADRUPOLE LENS

A Thesis
Submitted to the College of Science at
Al-Nahrain University in Partial Fulfillment of
the Requirements for the Degree of
Master of Science
in Physics

by
Fatma Nafaa Gaafer Al-Zubaidy
(B.Sc. 2004)

Moharam
February

1428 A.H.
2007 A.D.



جمهورية العراق
وزارة التعليم العالي والبحث العلمي
جامعة النهرين
كلية العلوم
قسم الفيزياء

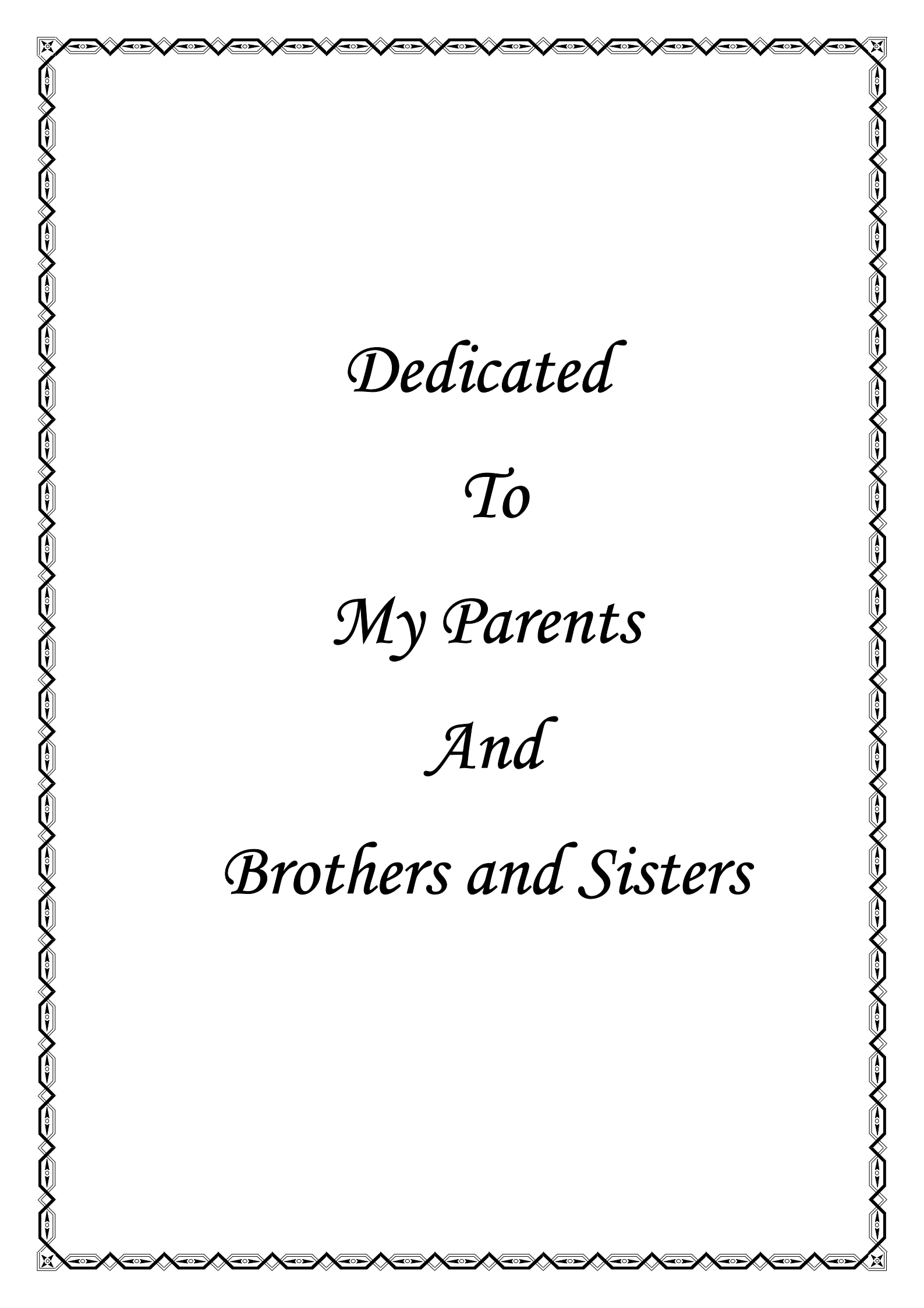
دراسة عن الخصائص البصرية لعدسة رباعية الاقطاب عديمة الزيغ اللوني

رسالة
مقدمة الى كلية العلوم في جامعة النهرين
وهي جزء من متطلبات نيل درجة
ماجستير علوم
في الفيزياء

أعداد
فاطمة نافع جعفر الزبيدي
(بكالوريوس ٢٠٠٤)

١٤٢٨ هـ
٢٠٠٧ م

محرم
شباط

A decorative border with a repeating geometric pattern of diamonds and circles surrounds the text.

Dedicated
To
My Parents
And
Brothers and Sisters

بِسْمِ اللَّهِ الرَّحْمَنِ الرَّحِيمِ

قَالُوا سُبْحَانَكَ لَا عِلْمَ لَنَا إِلَّا مَا عَلَّمْتَنَا إِنَّكَ أَنْتَ الْعَلِيمُ

الْحَكِيمُ

صدق الله العظيم

سورة البقرة

الآية (٣٢)